Resonant electron-atom bremsstrahlung in an intense laser field

A. N. Zheltukhin,[1,2] A. V. Flegel,[1,3] M. V. Frolov,[2] N. L. Manakov,[2] and Anthony F. Starace[1,*]
[1]*Department of Physics and Astronomy, The University of Nebraska, Lincoln, Nebraska 68588-0299, USA*
[2]*Department of Physics, Voronezh State University, Voronezh 394006, Russia*
[3]*Department of Computer Science, Voronezh State University, Voronezh 394006, Russia*
(Received 1 December 2013; published 7 February 2014)

We analyze a resonant mechanism for spontaneous laser-assisted electron bremsstrahlung (BrS) involving the resonant transition (via either laser-assisted electron-ion recombination or electron-atom attachment) into a laser-dressed intermediate quasibound state (corresponding, respectively, to either a field-free neutral atom or a negative-ion bound state) accompanied by ionization or detachment of this state by the laser field. This mechanism leads to resonant enhancement (by orders of magnitude) of the BrS spectral density for emitted photon energies corresponding to those for laser-assisted recombination or attachment. We present an accurate parametrization of the resonant BrS amplitude in terms of the amplitudes for nonresonant BrS, for recombination or attachment to the intermediate state, and for ionization or detachment of this state. The high accuracy of our general analytic parametrization of the resonant BrS cross section is shown by comparison with exact numerical results for laser-assisted BrS spectra obtained within time-dependent effective range theory. Numerical estimates of resonant BrS in electron scattering from a Coulomb potential are also presented.

DOI: 10.1103/PhysRevA.89.023407 PACS number(s): 34.80.Qb, 32.80.Qk, 03.65.Nk, 41.60.−m

I. INTRODUCTION

The bremsstrahlung (BrS) process accompanying electron-atom or electron-ion scattering is among the fundamental problems of atomic physics. In the presence of an intense laser field the BrS process is significantly modified: an electron colliding with an atom can efficiently convert the combined energies of the laser photons, $\hbar\omega$, into the energy of a spontaneously emitted photon, $\hbar\Omega$. In comparison with field-free BrS, in laser-assisted BrS the spectral energies can be significantly extended and resonant-like enhancements of the BrS cross sections may appear.

There have been relatively few prior studies of laser-assisted BrS processes. Karapetyan and Fedorov [1] have shown that laser-assisted BrS spectra for electron scattering from a Coulomb potential exhibit resonant peaks at BrS frequencies that are multiples of the laser frequency ω. Such resonances occur only in the limit of an intense laser field, i.e., such that the mean kinetic energy of free electron oscillations in the laser field is much higher than the incident electron energy. These results are apparently specifically for the long-range Coulomb potential. The electron-Coulomb interaction was treated in Ref. [1] within the Born approximation, so that effects related to the possibility of virtual capture of the scattering electron into a bound state were not treated.

Zhou and Rosenberg [2] investigated laser-assisted BrS beyond the Born approximation in the scattering potential for the case of a low-frequency laser field. They found a series of resonant peaks in the BrS spectrum, separated by $\hbar\omega$, that are related to resonant features in field-free electron-atom scattering. The approach in Ref. [2] is based on the low-frequency Kroll-Watson result [3] for the electron scattering state and its "resonant" modification, representing the scattering wave function in terms of the field-free continuum states with laser-modified energies. Within this low-frequency approximation, effects of the laser field on the resonant quasibound state of the electron in the atomic potential cannot be treated. Hence the low-frequency approach in Ref. [2] does not allow one to determine the correct field dependence of the resonant positions and profiles; they can only be introduced phenomenologically.

These two seminal works, by Karapetyan and Fedorov [1] and by Zhou and Rosenberg [2], have led to a number of more recent analyses. These have been described briefly in Sec. 4.5 of the review by Ehlotzky *et al.* [4]. A comparative analysis of laser-assisted BrS for electron-Coulomb scattering within the Born and low-frequency approximations (in accordance with Refs. [1] and [2], respectively) has been given in a recent paper by Dondera and Florescu [5], who also review there other works on nonrelativistic laser-assisted BrS.

In this paper, we analyze resonant effects in nonrelativistic laser-assisted BrS due to radiative transitions of the scattering electron into a bound state supported by the atomic potential. Our analysis goes beyond both the Born and the low-frequency approximations. We present a general parametrization for resonant BrS cross sections, which are expressed in terms of amplitudes for nonresonant BrS, for radiative recombination or attachment into a quasistationary bound state, and for ionization or detachment of the active electron from this state. This resonant channel (for virtual capture of the incident electron by the target potential) plays an important role in various collision processes, dramatically modifying the spectra of such processes. For example, significant enhancements of the cross sections for laser-assisted electron-atom scattering accompanied by absorption or emission of laser quanta was predicted in Ref. [6]. Also, the occurrence of resonant enhancements (by orders of magnitude) of the high-energy part of laser-assisted radiative recombination (LARR) or laser-assisted radiative attachment (LARA) spectra have been predicted in Ref. [7]. In this paper, we show (i) that the aforementioned resonant mechanism leads to the appearance of sharp resonant peaks in laser-assisted BrS spectra, increasing the BrS cross section by orders of magnitude; (ii) that the

*astarace1@unl.edu

 ©2014 American Physical Society

resonant peaks form a plateau-like structure, whose shape coincides with that of the LARR or LARA spectrum; and (iii) that the profiles of the resonant peaks are governed by the ratio of nonresonant (potential) to resonant BrS amplitudes and have an asymmetric form similar to the Fano profiles of autoionization features in photoionization cross sections (see Refs. [8–10]) as well as to the resonance profiles found in Ref. [7] for the LARR process. Note that in our treatment the resonant peak positions and widths are related to the Stark shift and the total decay rate of the resonant laser-dressed quasistationary bound state. Note also that our considerations are limited to the nonrelativistic case and to the dipole approximation for the electron interaction with the laser field; relativistic effects in laser-assisted BrS (cf., e.g., Refs. [11–14]) are beyond the scope of this paper.

The paper is organized as follows. In Sec. II we present a general formalism for laser-assisted resonant BrS for the case of electron scattering on a target potential that supports a bound state. We derive exact quantum expressions for the BrS cross section in the vicinity of the resonant energies of the emitted photon. In Sec. III we present closed-form analytic expressions (obtained within the low-frequency approximation) for the key contributions to the resonant BrS cross sections. In Sec. IV exact numerical results for laser-assisted resonant e-H BrS in a CO_2 laser field are presented. These are obtained using the time-dependent effective range theory (TDER) for an electron scattering state in a short-range atomic potential. In Sec. V, we present estimates for spontaneous laser-assisted BrS for the case of electron-Coulomb scattering. In Sec. VI we summarize our results and present some conclusions. Finally, in the Appendix we provide details of the derivation of the exact TDER result for the laser-assisted BrS amplitude.

II. GENERAL FORMALISM

A. The laser-assisted bremsstrahlung cross section

We consider the process of laser-assisted spontaneous photon emission (BrS) by a nonrelativistic electron that scatters from a target atom described by the potential $U(r)$. For the electron-laser interaction, we use the dipole approximation in the length gauge,

$$V(\mathbf{r},t) = -e\mathbf{r}\cdot\mathbf{F}(t),$$

where $\mathbf{F}(t)$ is the electric vector of the linearly polarized, monochromatic laser field,

$$\mathbf{F}(t) = \mathbf{F}\cos\omega t, \quad \mathbf{F} = \mathbf{e}_z F, \tag{1}$$

F and ω are the field amplitude and frequency, and $\mathbf{e}_z$ is the unit polarization vector.

To describe electron-atom collisions in a monochromatic field, (1), the quasienergy (or Floquet) approach [15] is most appropriate. Within this approach, the laser-dressed scattering state of an electron with asymptotic momentum $\mathbf{p}$ and kinetic energy $E = p^2/(2m)$ has the form

$$\Psi_{\mathbf{p}}(\mathbf{r},t) = \Phi_{\mathbf{p}}(\mathbf{r},t)e^{-i\epsilon t/\hbar}, \quad \Phi_{\mathbf{p}}(\mathbf{r},t) = \Phi_{\mathbf{p}}(\mathbf{r},t+T), \quad T = 2\pi/\omega, \tag{2}$$

where ϵ is the quasienergy, $\epsilon = E + u_p$, and $u_p = e^2F^2/(4m\omega^2)$ is the ponderomotive (or quiver) energy of an electron in the field $\mathbf{F}(t)$.

As for the case of field-free BrS [16], the amplitude for laser-assisted BrS is proportional to the matrix element (T_{fi}) of the dipole radiative transition between the initial ("in") and the final ("out") scattering states $\Psi^{(\mathrm{in})}_{\mathbf{p}_i}(\mathbf{r},t) = \Phi_{\mathbf{p}_i}(\mathbf{r},t)e^{-i\epsilon_i t/\hbar}$ and $\Psi^{(\mathrm{out})}_{\mathbf{p}_f}(\mathbf{r},t) = \Phi^{\mathcal{T}}_{\mathbf{p}_f}(\mathbf{r},t)e^{-i\epsilon_f t/\hbar}$, corresponding to the emission of a spontaneous photon with energy $\hbar\Omega$ and polarization vector $\mathbf{e}'$,

$$T_{fi} = \int_{-\infty}^{\infty} e^{i[\Omega-(\epsilon_i-\epsilon_f)/\hbar]t}\mathbf{e}'^{*}\cdot\mathbf{d}_{fi}(t)dt, \tag{3}$$

where $\mathbf{d}_{fi}(t)$ is the (periodic-in-time) matrix element of the dipole moment operator $\mathbf{d} = e\mathbf{r}$,

$$\mathbf{d}_{fi}(t) = \langle\Phi^{\mathcal{T}}_{\mathbf{p}_f}(t)|\mathbf{d}|\Phi_{\mathbf{p}_i}(t)\rangle. \tag{4}$$

In Eq. (4), the in state, $\Phi_{\mathbf{p}_i}(t) \equiv \Phi_{\mathbf{p}_i}(\mathbf{r},t)$, contains incoming "plane" and outgoing "spherical" waves, whereas the out state, $\Phi^{\mathcal{T}}_{\mathbf{p}_f}(t) \equiv \Phi^{\mathcal{T}}_{\mathbf{p}_f}(\mathbf{r},t)$, contains outgoing plane and incoming spherical waves and relates to the quasienergy state (QES) $\Phi_{\mathbf{p}_f}(\mathbf{r},t)$ as

$$\Phi^{\mathcal{T}}_{\mathbf{p}_f}(\mathbf{r},t) = \Phi^{*}_{-\mathbf{p}_f}(\mathbf{r},-t). \tag{5}$$

Using the Fourier expansion for $\mathbf{d}_{fi}(t)$, the integration over t in Eq. (3) gives

$$T_{fi} = 2\pi\hbar\sum_n \mathbf{e}'^{*}\cdot\mathbf{d}_n\delta(\epsilon_i + n\hbar\omega - \hbar\Omega - \epsilon_f), \tag{6}$$

where $\mathbf{d}_n = \mathbf{d}_n(\mathbf{p}_i,\mathbf{p}_f)$ is the Fourier component of $\mathbf{d}_{fi}(t)$:

$$\mathbf{d}_n(\mathbf{p}_i,\mathbf{p}_f) = \frac{1}{T}\int_0^T dt e^{in\omega t}\langle\Phi^{\mathcal{T}}_{\mathbf{p}_f}(t)|\mathbf{d}|\Phi_{\mathbf{p}_i}(t)\rangle. \tag{7}$$

The δ functions in Eq. (6) determine the relation between the spontaneous photon energy and the number n of laser photons exchanged:

$$\hbar\Omega = \frac{p_i^2 - p_f^2}{2m} + n\hbar\omega. \tag{8}$$

For a given n, the BrS doubly differential cross section with respect to the emitted photon frequency Ω and the final electron direction (we denote the corresponding solid angle element as $d\Omega_{\mathbf{p}_f}$), summed over polarizations and integrated over directions of the emitted photon, has the following form:

$$\frac{d^2\sigma_n(\mathbf{p}_i,\mathbf{p}_f)}{d\Omega d\Omega_{\mathbf{p}_f}} = \frac{\Omega^3 m^2}{6(\pi\hbar c)^3}\frac{p_f}{p_i}|\mathbf{d}_n(\mathbf{p}_i,\mathbf{p}_f)|^2. \tag{9}$$

For $\mathbf{F}(t) = 0$, the matrix element, (7), reduces to that for field-free BrS, $\langle\varphi^{(-)}_{\mathbf{p}_f}|\mathbf{d}|\varphi^{(+)}_{\mathbf{p}_i}\rangle$ (where $\varphi^{(+)}_{\mathbf{p}_i}$ and $\varphi^{(-)}_{\mathbf{p}_f}$ are field-free in and out scattering states), so that the result, (9), for this case coincides with the doubly differential cross section for field-free BrS [16]. Summing the partial "n-photon" cross sections $d^2\sigma_n/d\Omega d\Omega_{\mathbf{p}_f}$ over n and integrating over the directions of the final electron momentum $\mathbf{p}_f$, we obtain, for the angle-integrated BrS cross section (or "spectral density"),

$$\frac{d\sigma(\mathbf{p}_i,\Omega)}{d\Omega} = \frac{\Omega^3 m^2}{6(\pi\hbar c)^3}\sum_{n>\xi}^{\infty}\int d\Omega_{\mathbf{p}_f}\frac{p_f}{p_i}|\mathbf{d}_n(\mathbf{p}_i,\mathbf{p}_f)|^2, \tag{10}$$

where $\xi = \Omega/\omega - p_i^2/(2m\hbar\omega)$, so that the summation over n involves all open channels (for which $p_f^2 > 0$).

B. Resonant bremsstrahlung

We assume that the scattering potential $U(r)$ supports a bound state $\varphi_{E_0}(\mathbf{r})$ with energy E_0, which evolves in the laser field to the quasistationary quasienergy state (QQES) $\Phi_\varepsilon(\mathbf{r},t)$. The wave function $\Phi_\varepsilon(\mathbf{r},t)$ is similar to $\Phi_\mathbf{p}(\mathbf{r},t)$ in Eq. (2), but with the complex quasienergy $\varepsilon = E_0 + \Delta E_0 - i\Gamma/2$, where ΔE_0 and Γ are the field-induced Stark shift and width (or total decay rate $\Gamma/\hbar$) of state $\varphi_{E_0}(\mathbf{r})$ [15].

For a spontaneous BrS photon frequency $\Omega \approx \Omega_\mu$, where μ is an integer and

$$\hbar\Omega_\mu = \epsilon_i - \mathrm{Re}\,\varepsilon + \mu\hbar\omega, \tag{11}$$

the BrS process is resonant: upon absorbing μ laser photons, followed by emission of a spontaneous photon of frequency Ω_μ, the electron can be virtually captured into the quasibound state $\Phi_\varepsilon(\mathbf{r},t)$ (as in LARA or LARR), followed by detachment or ionization of state $\Phi_\varepsilon(\mathbf{r},t)$ with absorption of $\nu = n - \mu$ photons. Both nonresonant and resonant BrS channels are shown schematically in Fig. 1.

Our analysis of resonant BrS is based on the fact that, for any integer $\nu > (|\mathrm{Re}\,\varepsilon| + u_p)/(\hbar\omega)$ and small Γ ($\Gamma \ll |\mathrm{Re}\,\varepsilon|$), the QES wave function $\Phi_\mathbf{p}(\mathbf{r},t)$ has singularities at the resonant quasienergies ϵ_ν [17], where

$$\epsilon_\nu = \mathrm{Re}\,\varepsilon + \nu\hbar\omega. \tag{12}$$

The general form of the scattering QES in the vicinity of the resonant energy ϵ_ν is considered next.

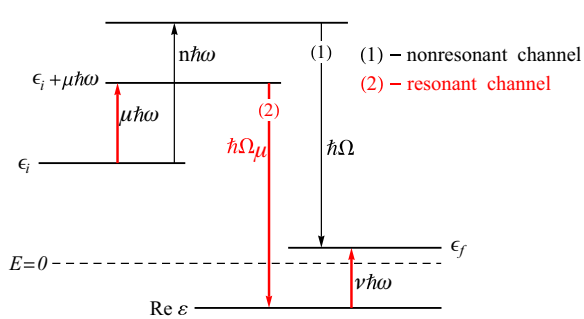

FIG. 1. (Color online) Schematic for electron-atom BrS in a strong monochromatic laser field, indicating both nonresonant and resonant channels for an electron initially in the quasienergy state (QES) with quasienergy ϵ_i and, finally, in the QES with quasienergy ϵ_f. Thin (black) arrows indicate a nonresonant BrS channel involving absorption of n laser photons with energy $\hbar\omega$ and emission of a BrS photon [arrow (1)] with energy $\hbar\Omega$. Thick (red) arrows indicate a resonant channel involving absorption of μ laser photons, emission of a BrS photon [arrow (2)] with energy $\hbar\Omega_\mu = \hbar\Omega$ to a bound quasistationary quasienergy state (QQES) with complex energy ε, and ionization with absorption of ν ($= n - \mu$) laser photons. See text for discussion.

C. Scattering states with near-resonant energies

The scattering QES wave functions satisfy the Lippmann-Schwinger equation:

$$\Phi_\mathbf{p}(\mathbf{r},t) = \chi_\mathbf{p}(\mathbf{r},t) + \frac{1}{T}\int_0^T dt' \int d\mathbf{r}'\mathcal{G}_\epsilon(\mathbf{r},t,\mathbf{r}',t') \times U(r')\Phi_\mathbf{p}(\mathbf{r}',t'). \tag{13}$$

Here $\chi_\mathbf{p}(\mathbf{r},t)$ is the QES wave function of a free electron with momentum $\mathbf{p}$ in the laser field (i.e., the time-periodic part of a Volkov wave function),

$$\chi_\mathbf{p}(\mathbf{r},t) = e^{i[\mathbf{P}(t)\mathbf{r} + S_\mathbf{p}(t)]/\hbar}, \tag{14}$$

where

$$S_\mathbf{p}(t) = -\int^t [\mathbf{P}^2(\tau)/(2m) - \epsilon]d\tau = \frac{e\mathbf{p}\cdot\mathbf{F}}{m\omega^2}\cos\omega t + \frac{u_p}{2\omega}\sin 2\omega t, \tag{15}$$

and $\mathbf{P}(t) = \mathbf{p} - (e/c)\mathbf{A}(t)$ is the electron's kinetic momentum in the laser field $\mathbf{F}(t)$ with vector potential $\mathbf{A}(t) = -(c\mathbf{F}/\omega)\sin\omega t$. Also, in Eq. (13) $\mathcal{G}_\epsilon(\mathbf{r},t,\mathbf{r}',t')$ is the quasienergy (time-periodic) retarded Green's function for a free electron in the laser field $\mathbf{F}(t)$ [17],

$$\mathcal{G}_\epsilon(\mathbf{r},t,\mathbf{r}',t') = \sum_{s=-\infty}^{\infty}\int d\mathbf{q}\frac{e^{is\omega(t-t')}\chi_\mathbf{q}(\mathbf{r},t)\chi_\mathbf{q}^*(\mathbf{r}',t')}{(2\pi\hbar)^3[\epsilon - \epsilon_q - s\hbar\omega + i0]}, \tag{16}$$

where $\epsilon_q = q^2/(2m) + u_p$.

Substituting Fourier series expansions for the time-periodic functions $\Phi_\mathbf{p}(\mathbf{r},t)$ and $\chi_\mathbf{p}(\mathbf{r},t)$,

$$\Phi_\mathbf{p}(\mathbf{r},t) = \sum_k e^{-ik\omega t}\Phi_{\mathbf{p},k}(\mathbf{r}),$$

$$\chi_\mathbf{p}(\mathbf{r},t) = \sum_k e^{-ik\omega t}\chi_{\mathbf{p},k}(\mathbf{r}),$$

into Eqs. (13) and (16), we obtain the following system of equations for the Fourier components $\Phi_{\mathbf{p},k}(\mathbf{r})$:

$$\Phi_{\mathbf{p},n}(\mathbf{r}) = \chi_{\mathbf{p},n}(\mathbf{r}) + \sum_k\int d\mathbf{r}' M_{n,k}(\epsilon,\mathbf{r},\mathbf{r}')U(r')\Phi_{\mathbf{p},k}(\mathbf{r}'), \tag{17}$$

where the functions $M_{n,k}(\epsilon,\mathbf{r},\mathbf{r}')$ are defined by

$$M_{n,k}(\epsilon,\mathbf{r},\mathbf{r}') = \sum_{s=-\infty}^{\infty}\int d\mathbf{q}\frac{\chi_{\mathbf{q},s+n}(\mathbf{r})\chi_{\mathbf{q},s+k}^*(\mathbf{r}')}{(2\pi\hbar)^3[\epsilon - \epsilon_q - s\hbar\omega + i0]}. \tag{18}$$

From the explicit form of $M_{n,k}(\epsilon,\mathbf{r},\mathbf{r}')$, we note the following symmetry relation:

$$M_{n,k}(\epsilon + \nu\hbar\omega,\mathbf{r},\mathbf{r}') = M_{n+\nu,k+\nu}(\epsilon,\mathbf{r},\mathbf{r}'). \tag{19}$$

It is well known that the complex quasienergy ε can be obtained as the pole of the QES wave function $\Phi_\mathbf{p}(\mathbf{r},t)$ in the complex plane of quasienergy ϵ, while the residue of the function $\Phi_\mathbf{p}(\mathbf{r},t)$ at this pole is proportional to the QQES wave function $\Phi_\varepsilon(\mathbf{r},t)$ [15,17]. Thus near the resonant energy ϵ_ν, defined by Eq. (12), the QES wave function can

be approximated as the sum of potential (nonresonant) and resonant parts,

$$\Phi_{\mathbf{p}}(\mathbf{r},t) = \Phi^{(p)}_{\mathbf{p}_\nu}(\mathbf{r},t) + \Phi^{(r)}_{\mathbf{p}}(\mathbf{r},t), \tag{20}$$

where $\mathbf{p}_\nu$ is the "resonant momentum":

$$\mathbf{p}_\nu = \hat{\mathbf{p}}\sqrt{2m(\epsilon_\nu - u_p)}, \quad \hat{\mathbf{p}} = \mathbf{p}/p. \tag{21}$$

In accordance with the discussion above, the resonant part of the QES $\Phi_{\mathbf{p}}(\mathbf{r},t)$ is approximated by

$$\Phi^{(r)}_{\mathbf{p}}(\mathbf{r},t) = \alpha(\mathbf{p})\Phi_\varepsilon(\mathbf{r},t)e^{i\nu\omega t}, \tag{22}$$

where $\alpha(\mathbf{p})$ has to be determined. Note that the Fourier components $\Phi_{\varepsilon,k}(\mathbf{r})$ of the QQES $\Phi_\varepsilon(\mathbf{r},t)$ [where $\Phi_{\varepsilon,k}(\mathbf{r}) = T^{-1}\int_0^T e^{ik\omega t}\Phi_\varepsilon(\mathbf{r},t)dt$] satisfy the homogeneous system of equations,

$$\Phi_{\varepsilon,n}(\mathbf{r}) = \sum_k \int d\mathbf{r}' M_{n,k}(\varepsilon,\mathbf{r},\mathbf{r}')U(r')\Phi_{\varepsilon,k}(\mathbf{r}'). \tag{23}$$

To find $\alpha(\mathbf{p})$, which enters into Eq. (22), we solve system (17) for $\Phi_{\mathbf{p},n}$ near resonance, i.e., for $\epsilon \approx \varepsilon + \nu\hbar\omega$. Expanding the functions $M_{n,k}(\epsilon,\mathbf{r},\mathbf{r}')$ up to the linear term in $\Delta\epsilon = \epsilon - \epsilon_\nu + i\Gamma/2$, and taking into account the symmetry relation, (19), we obtain

$$\begin{aligned}\Phi_{\mathbf{p},n-\nu}(\mathbf{r}) &= \chi_{\mathbf{p},n-\nu}(\mathbf{r}) \\ &\quad + \sum_k \int d\mathbf{r}' M_{n,k}(\varepsilon,\mathbf{r},\mathbf{r}')U(r')\Phi_{\mathbf{p},k-\nu}(\mathbf{r}') \\ &\quad + \Delta\epsilon \sum_k \int d\mathbf{r}' M'_{n,k}(\varepsilon,\mathbf{r},\mathbf{r}')U(r')\Phi_{\mathbf{p},k-\nu}(\mathbf{r}'),\end{aligned} \tag{24}$$

where $M'_{n,k}(\varepsilon,\mathbf{r},\mathbf{r}') = \partial M_{n,k}(\epsilon,\mathbf{r},\mathbf{r}')/\partial\epsilon|_{\epsilon=\varepsilon}$. Considering the lowest resonant approximation ($|\Delta\epsilon| \to 0$), we neglect the potential part of the scattering QES in Eq. (20) and approximate $\chi_{\mathbf{p},n}(\mathbf{r})$ by its value at $\mathbf{p} = \mathbf{p}_\nu$:

$$\Phi_{\mathbf{p},n-\nu}(\mathbf{r}) \approx \Phi^{(r)}_{\mathbf{p},n-\nu}(\mathbf{r}) = \alpha(\mathbf{p})\Phi_{\varepsilon,n}(\mathbf{r}), \tag{25}$$

$$\chi_{\mathbf{p},n-\nu}(\mathbf{r}) \approx \chi_{\mathbf{p}_\nu,n-\nu}(\mathbf{r}). \tag{26}$$

Substituting Eqs. (25) and (26) into Eq. (24) and taking into account Eq. (23), we obtain the equation for $\alpha(\mathbf{p})$:

$$\begin{aligned}&\alpha(\mathbf{p})\Delta\epsilon \sum_k \int d\mathbf{r}' M'_{n,k}(\varepsilon,\mathbf{r},\mathbf{r}')U(r')\Phi_{\varepsilon,k}(\mathbf{r}) \\ &\quad + \chi_{\mathbf{p}_\nu,n-\nu}(\mathbf{r}) = 0.\end{aligned} \tag{27}$$

Finally, multiplying Eq. (27) by $\Phi_{\varepsilon,n}(\mathbf{r})U(r)$, integrating over $\mathbf{r}$, and summing over n, we find

$$\alpha(\mathbf{p}) = -\frac{2\pi\hbar^2}{m}\frac{\mathcal{N}^{-1}A^{(\mathrm{att})}_\nu(\mathbf{p}_\nu)}{\epsilon - \epsilon_\nu + i\Gamma/2}, \tag{28}$$

where $A^{(\mathrm{att})}_\nu(\mathbf{p}_\nu)$ is the amplitude for ν-photon laser-stimulated attachment or recombination, which is related to the amplitude $A^{(\mathrm{det})}_\nu(\mathbf{p}_\nu)$ for laser-induced detachment or ionization by $A^{(\mathrm{att})}_\nu(\mathbf{p}_\nu) = A^{(\mathrm{det})}_\nu(-\mathbf{p}_\nu)$, where

$$A^{(\mathrm{det})}_\nu(\mathbf{p}_\nu) = \frac{-m}{2\pi\hbar^2 T}\int_0^T dt e^{i\nu\omega t}\langle\chi_{\mathbf{p}_\nu}(t)|U|\Phi_\varepsilon(t)\rangle. \tag{29}$$

In Eq. (28) we have introduced the notation

$$\begin{aligned}\mathcal{N} = -\sum_{n,k}\int d\mathbf{r}\int d\mathbf{r}' M'_{n,k}(\varepsilon,\mathbf{r},\mathbf{r}') \\ \times U(r')\Phi_{\varepsilon,k}(\mathbf{r}')U(r)\Phi_{\varepsilon,n}(\mathbf{r}).\end{aligned} \tag{30}$$

It can be shown that the factor $\mathcal{N}$, given by Eq. (30), is equal to the norm of the QQES $\Phi_\varepsilon(\mathbf{r},t)$. First, we introduce the function $\Phi^{\mathcal{T}}_\varepsilon(\mathbf{r},t)$,

$$\Phi^{\mathcal{T}}_\varepsilon(\mathbf{r},t) = \Phi^*_\varepsilon(\mathbf{r},-t),$$

which enters the normalization condition for $\Phi_\varepsilon(\mathbf{r},t)$ [18],

$$\frac{1}{T}\int_0^T dt\langle\Phi^{\mathcal{T}}_\varepsilon(t)|\Phi_\varepsilon(t)\rangle = \sum_n\langle\Phi^{\mathcal{T}}_{\varepsilon,n}|\Phi_{\varepsilon,n}\rangle = 1. \tag{31}$$

By substituting Eq. (23) into the term $\sum_n\langle\Phi^{\mathcal{T}}_{\varepsilon,n}|\Phi_{\varepsilon,n}\rangle$ in Eq. (31) and taking into account the explicit form, (18), for the functions $M_{n,k}$, this term can be transformed to the form of (30), showing that $\mathcal{N} = 1$.

As a result, we obtain that the QES wave function near resonant energies has the form

$$\Phi_{\mathbf{p}}(\mathbf{r},t) = \Phi^{(p)}_{\mathbf{p}_\nu}(\mathbf{r},t) - \frac{2\pi\hbar^2}{m}A^{(\mathrm{att})}_\nu(\mathbf{p}_\nu)\frac{\Phi_\varepsilon(\mathbf{r},t)e^{i\nu\omega t}}{\epsilon - \epsilon_\nu + i\Gamma/2}. \tag{32}$$

D. General parametrization of the BrS cross section near resonant frequencies Ω_μ

The BrS matrix element $\mathbf{d}_n(\mathbf{p}_i,\mathbf{p}_f)$ in Eq. (7) in the neighborhood of a resonant frequency Ω_μ, given by Eq. (11), can be found by substituting the wave function $\Phi_{\mathbf{p}_f}(\mathbf{r},t)$ of the final QES in the form of (32) into Eq. (7). This allows one to express $\mathbf{d}_n(\mathbf{p}_i,\mathbf{p}_f)$ as the sum of potential and resonant terms,

$$\begin{aligned}\mathbf{d}_n(\mathbf{p}_i,\mathbf{p}_f) &= \mathbf{d}^{(p)}_n(\mathbf{p}_i,\mathbf{p}_\nu) + \frac{\mathbf{d}^{(r)}_n(\mathbf{p}_i,\mathbf{p}_\nu)}{\delta + i}, \\ \delta &= 2\Gamma^{-1}(\epsilon_f - \epsilon_\nu) = 2\hbar\Gamma^{-1}(\Omega_\mu - \Omega),\end{aligned} \tag{33}$$

where the resonant quasienergy ϵ_ν and momentum $\mathbf{p}_\nu$ of the final state are defined in Eqs. (12) and (21), respectively. The potential term $\mathbf{d}^{(p)}_n$ in Eq. (33) is given by Eq. (7) [upon substituting $\Phi^{(p)}_{\mathbf{p}_\nu}(\mathbf{r},t)$ for $\Phi_{\mathbf{p}_f}(\mathbf{r},t)$ there]. The resonant term involves the vector $\mathbf{d}^{(r)}_n$,

$$\mathbf{d}^{(r)}_n(\mathbf{p}_i,\mathbf{p}_\nu) = -\frac{4\pi\hbar^2}{m\Gamma}\tilde{\mathbf{d}}_\mu(\mathbf{p}_i)\,A^{(\mathrm{det})}_\nu(\mathbf{p}_\nu)\delta_{n,\nu+\mu},$$

expressed in terms of the dipole moment $\tilde{\mathbf{d}}_\mu$ for LARA or LARR accompanied by absorption of μ photons:

$$\tilde{\mathbf{d}}_\mu(\mathbf{p}) = \frac{1}{T}\int_0^T dt e^{i\mu\omega t}\langle\Phi^{\mathcal{T}}_\varepsilon(t)|\mathbf{d}|\Phi_{\mathbf{p}}(t)\rangle.$$

Substituting $\mathbf{d}_n$ in the form of (33) into Eq. (9) for the BrS cross section $d^2\sigma_n/d\Omega d\Omega_{\mathbf{p}_f}$ in the vicinity of $\Omega \approx \Omega_\mu$, we obtain

$$\frac{d^2\sigma_n(\Omega)}{d\Omega d\Omega_{\mathbf{p}_f}} = \frac{d^2\sigma^{(p)}_n(\Omega_\mu)}{d\Omega d\Omega_{\mathbf{p}_f}} + \frac{d^2\sigma^{(r)}_n(\Omega)}{d\Omega d\Omega_{\mathbf{p}_f}}, \tag{34}$$

where $d^2\sigma_n^{(p)}/d\Omega d\Omega_{\mathbf{p}_f}$ is the potential part of the BrS cross section, given by Eq. (9) upon substituting $\mathbf{d}_n \to \mathbf{d}_n^{(p)}$ there. The resonant part of the BrS cross section is

$$\frac{d^2\sigma_n^{(r)}}{d\Omega d\Omega_{\mathbf{p}_f}} = \widetilde{\sigma}_\mu(\mathbf{p}_i)\frac{dR(\mathbf{p}_\nu)}{d\Omega_{\mathbf{p}_\nu}}\frac{2\hbar^2}{\pi\Gamma^2}\frac{1+\mathrm{Im}\,q+\delta\mathrm{Re}\,q}{\delta^2+1}\delta_{n,\nu+\mu}, \tag{35}$$

where $\widetilde{\sigma}_\mu(\mathbf{p})$ is the LARA or LARR cross section,

$$\widetilde{\sigma}_\mu(\mathbf{p}) = \frac{4m\Omega_\mu^3}{3\hbar c^3 p}|\widetilde{\mathbf{d}}_\mu(\mathbf{p})|^2, \tag{36}$$

$dR/d\Omega_{\mathbf{p}_\nu}$ is the differential rate of laser-induced ν-photon detachment or ionization,

$$\frac{dR(\mathbf{p}_\nu)}{d\Omega_{\mathbf{p}_\nu}} = \frac{p_\nu}{m}\left|A_\nu^{(\mathrm{det})}(\mathbf{p}_\nu)\right|^2, \tag{37}$$

and the Fano-type asymmetry parameter q (similar to the Fano parameter describing autoionization features in photoionization cross sections [8–10]) has the form

$$q = 2\mathbf{d}_n^{(p)*}\cdot\mathbf{d}_n^{(r)}\big/\left|\mathbf{d}_n^{(r)}\right|^2. \tag{38}$$

Results (34) and (35) show that the cross section $d^2\sigma_n^{(r)}(\Omega)/d\Omega d\Omega_{\mathbf{p}_f}$ as a function of the spontaneous photon frequency is asymmetric with respect to the resonant frequency Ω_μ. This is similar to the incident electron energy dependence of the LARA or LARR cross section (cf. Ref. [7]).

Neglecting in Eq. (34) the (nonresonant) potential term, summing over the final electron energies ϵ_ν [cf. Eq. (12)], and integrating over the directions of the final momentum $\mathbf{p}_f = \mathbf{p}_\nu$, one obtains, for the resonant BrS cross section,

$$\frac{d\sigma^{(\mu)}(\Omega)}{d\Omega} = \sum_{\nu=\nu_{\min}}^{\infty}\int d\Omega_{\mathbf{p}_\nu}\frac{d^2\sigma_{\mu+\nu}^{(r)}}{d\Omega d\Omega_{\mathbf{p}_\nu}} = \frac{2\hbar}{\pi\Gamma}\frac{\widetilde{\sigma}_\mu(\mathbf{p}_i)}{\delta^2+1}, \tag{39}$$

where the summation over ν involves open channels with $p_\nu^2 > 0$. To obtain result (39) we have used the following expression for the total ionization rate:

$$\sum_{\nu=\nu_{\min}}^{\infty}\int d\Omega_{\mathbf{p}_\nu}\frac{dR(\mathbf{p}_\nu)}{d\Omega_{\mathbf{p}_\nu}} = \frac{\Gamma}{\hbar}. \tag{40}$$

After integration of the resonant BrS cross section $d\sigma^{(\mu)}/d\Omega$ in Eq. (39) over the neighborhood of $\Omega = \Omega_\mu$ ($\Omega_\mu - \omega/2 < \Omega < \Omega_\mu + \omega/2$, where $\omega \gg \Gamma/\hbar$), the total resonant BrS cross section is equal to the μ-photon LARA or LARR cross section $\widetilde{\sigma}_\mu(\mathbf{p}_i)$:

$$\int_{\Omega_\mu-\omega/2}^{\Omega_\mu+\omega/2} d\Omega\frac{d\sigma^{(\mu)}(\Omega)}{d\Omega} \approx \frac{\widetilde{\sigma}_\mu(\mathbf{p}_i)}{\pi}\int_{-\infty}^{\infty}\frac{d\delta}{\delta^2+1} = \widetilde{\sigma}_\mu(\mathbf{p}_i). \tag{41}$$

Equations (34) and (35) represent the key results for the laser-assisted BrS cross section near resonant frequencies $\Omega \approx \Omega_\mu$. In particular, these results show explicitly that the process of spontaneous photon emission by a continuum electron interacting with a potential includes a resonant channel involving the formation of a virtual bound state of the target potential $U(r)$. Moreover, Eq. (35) shows that the resonant BrS cross section $d^2\sigma_n^{(r)}/d\Omega d\Omega_{\mathbf{p}_f}$ has a factorized form with two factors: the factor $\widetilde{\sigma}_\mu$, describing radiative attachment or recombination to the virtual bound state; and the factor $dR/d\Omega_{\mathbf{p}_\nu}$, describing detachment or ionization of the virtual bound state.

III. RESONANT BREMSSTRAHLUNG IN A LOW-FREQUENCY LASER FIELD

The results of the previous section in Eqs. (34)–(38) show that the resonant BrS cross section is completely determined by the following key ingredients: (i) the dipole moment for nonresonant laser-assisted BrS, $\mathbf{d}_n^{(p)}$ [which determines the potential part, $d^2\sigma_n^{(p)}/d\Omega d\Omega_{\mathbf{p}_f}$, of the BrS cross section in Eq. (34) and contributes to the asymmetry parameter q, given by Eq. (38)]; (ii) the dipole moment for LARA or LARR, $\widetilde{\mathbf{d}}_\mu$ [which determines the LARA or LARR cross section, $\widetilde{\sigma}_\mu$, in Eq. (36), and also contributes to the parameter q]; and (iii) the amplitude for detachment or ionization from the virtual bound state, $A_\nu^{(\mathrm{det})}$ [cf. Eq. (37)].

In the case of a low-frequency laser field, the aforementioned quantities have closed-form analytic expressions, from each of which one can factor out the dependence on the details of the electron-atom dynamics. Typically when one makes the low-frequency approximation, one assumes that the electron-atom interaction, $U(r)$, is of short range. For a long-range interaction, $U(r)$ (e.g., for a Coulomb potential), the derivation of a low-frequency approximation requires a careful analysis. In general, the atomic factors for the case of a short-range interaction can be replaced by their "long-range" counterparts, which is justified when interference between amplitudes for different channels of the process is negligibly small. (In this case one can neglect the details of the electron-atom interaction in the phase factors of the complex amplitudes.) For the case of resonant BrS, in which there is strong interference between the resonant and the potential channels [especially if the absolute values of $\mathbf{d}_n^{(r)}$ and $\mathbf{d}_n^{(p)}$ are comparable], the dependence of the phase factors of $\mathbf{d}_n^{(r)}$ and $\mathbf{d}_n^{(p)}$ on the atomic dynamics is important. In particular, the real and imaginary parts of the asymmetry parameter q in the resonant part of the BrS cross section in Eq. (35) (which determine the profile of the resonant peak) depend on the characteristics of the electron-atom interaction and may differ for short-range and long-range interactions $U(r)$.

Below we present analytic results for the key ingredients of the resonant BrS cross section, obtained for the case of a short-range potential.

A. Low-frequency results for nonresonant BrS and the classical limit

The process of laser-assisted BrS in the case of a low-frequency laser field without taking into account the possibility of virtual attachment of the active electron to the target atom potential (followed by detachment) was considered in Ref. [2]. Briefly, the initial $\Phi_{\mathbf{p}_i}$ and final $\Phi_{\mathbf{p}_f}$ QESs in Eq. (7) are treated within the Kroll-Watson approximation [3] for the electron scattering state,

$$\Phi_{\mathbf{p}}(\mathbf{r},t) \approx \Phi_{\mathbf{p}}^{(\mathrm{KW})}(\mathbf{r},t) = \varphi_{\mathbf{P}(t)}(\mathbf{r})e^{iS_{\mathbf{p}}(t)/\hbar}, \tag{42}$$

where $\varphi_{\mathbf{P}(t)}(\mathbf{r})$ is the field-free scattering state of an electron in the potential $U(r)$ with laser-modified kinetic momentum $\mathbf{P}(t)$, and the classical action $S_{\mathbf{p}}(t)$ is defined in Eq. (15). With the QES wave functions $\Phi_{\mathbf{p}_i}$ and $\Phi_{\mathbf{p}_f}$ in the form of (42), one obtains, for the potential part $\mathbf{d}_n^{(p)}$ of the BrS amplitude, the Zhou-Rosenberg result [2],

$$\mathbf{d}_n^{(p)}(\mathbf{p}_i,\mathbf{p}_f) = \frac{1}{T}\int_0^T dt e^{in\omega t + i\rho\cos\omega t}\mathbf{d}^{(0)}(\mathbf{P}_i(t),\mathbf{P}_f(t)), \quad (43)$$

where

$$\rho = e\mathbf{F}\cdot(\mathbf{p}_i - \mathbf{p}_f)/(m\hbar\omega^2), \quad (44)$$

and $\mathbf{d}^{(0)}(\mathbf{P}_i,\mathbf{P}_f)$ is the field-free BrS matrix element,

$$\mathbf{d}^{(0)}(\mathbf{P}_i(t),\mathbf{P}_f(t)) = \langle\varphi^{\mathcal{T}}_{\mathbf{P}_f(t)}|\mathbf{d}|\varphi_{\mathbf{P}_i(t)}\rangle,$$

involving laser-modified initial and final kinetic momenta, $\mathbf{P}_{i,f}(t) = \mathbf{p}_{i,f} - (e/c)\mathbf{A}(t)$.

In the low-frequency limit, we assume $\mathbf{d}^{(0)}(\mathbf{P}_i(t),\mathbf{P}_f(t))$ to be a slowly varying function of t, while the exponential factor in the integrand of Eq. (43) oscillates rapidly. Hence, we approximate result (43) by factoring $\mathbf{d}^{(0)}(\mathbf{P}_i(t),\mathbf{P}_f(t))$ out of the integral at a saddle point $t = t_0$, followed by analytic evaluation of the remaining integral in terms of a Bessel function. Thus we obtain

$$\mathbf{d}_n^{(p)}(\mathbf{p}_i,\mathbf{p}_f) = i^n J_n(\rho)\,\mathbf{d}^{(0)}(\mathbf{P}_i(t_0),\mathbf{P}_f(t_0)), \quad (45)$$

where $J_n(\rho)$ is the ordinary Bessel function, and the saddle point t_0 satisfies the equation

$$\rho\sin\omega t_0 = n. \quad (46)$$

Equation (46) can be rewritten in the form

$$\left[\mathbf{P}_i^2(t_0) - \mathbf{P}_f^2(t_0)\right]/(2m) = \hbar\Omega, \quad (47)$$

which ensures energy conservation at the time of spontaneous photon emission.

Substituting the low-frequency result, (45), into Eq. (9), we obtain, for the BrS double-differential cross section,

$$\frac{d^2\sigma_n^{(p)}(\mathbf{p}_i,\mathbf{p}_f)}{d\Omega d\Omega_{\mathbf{p}_f}} = \frac{P_i p_f}{p_i P_f} J_n^2(\rho)\frac{d^2\sigma^{(0)}(\mathbf{P}_i,\mathbf{P}_f)}{d\Omega d\Omega_{\mathbf{P}_f}}, \quad (48)$$

where $P_{i,f} \equiv |\mathbf{P}_{i,f}(t_0)|$, and $d^2\sigma^{(0)}/d\Omega d\Omega_{\mathbf{P}_f}$ is the field-free BrS cross section.

The low-frequency results, (45) and (48), are factorized expressions, where the field-free quantities [$\mathbf{d}^{(0)}$ and $d^2\sigma^{(0)}/d\Omega d\Omega_{\mathbf{P}_f}$] contain the complete information on the atomic dynamics. (This factorization is similar to the Kroll-Watson result for laser-assisted electron scattering cross sections [3].) The field-free cross section $d^2\sigma^{(0)}/d\Omega d\Omega_{\mathbf{P}_f}$ in Eq. (48) is a smooth function of the number n of absorbed laser photons, depending on n only through its implicit dependence on the solution $t_0(n)$ of Eq. (46). The Bessel function $J_n(\rho)$ determines for the most part the shape of the nonresonant BrS spectrum. As is well known, $J_n(\rho)$ oscillates as a function of n in the range $|n| < |\rho|$ [in which the saddle point equation, (46), has only real solutions] and decays exponentially for $|n| > |\rho|$. Thus, Eq. (48) describes a plateau-like structure for spontaneous photon frequencies in the interval $\Omega_-^{(p)} < \Omega < \Omega_+^{(p)}$, where

$$\hbar\Omega_\pm^{(p)} = \frac{p_i^2 - p_f^2}{2m} \pm \frac{|e\mathbf{F}\cdot(\mathbf{p}_i - \mathbf{p}_f)|}{m\omega}. \quad (49)$$

For parameters such that Eq. (49) gives $\Omega_-^{(p)} < 0$, we set $\Omega_-^{(p)} = 0$. In the case $\Omega_+^{(p)} < 0$, nonresonant BrS is classically forbidden, so that the plateau in the nonresonant BrS spectrum disappears.

The low-frequency result for the potential part of the BrS spectral density, (10), is thus

$$\frac{d\sigma^{(p)}(\mathbf{p}_i,\Omega)}{d\Omega} = \sum_{n>\xi}^{\infty}\int d\Omega_{\mathbf{p}_f}\frac{P_i p_f}{p_i P_f}J_n^2(\rho)\frac{d^2\sigma^{(0)}(\mathbf{P}_i,\mathbf{P}_f)}{d\Omega d\Omega_{\mathbf{P}_f}}. \quad (50)$$

Owing to the Bessel functions in Eq. (50), the spectral density as a function of Ω exhibits a plateau-like structure in the BrS spectrum for $0 < \Omega < \Omega_{\max}^{(p)}$. The cutoff position of this plateau, $\hbar\Omega_{\max}^{(p)}$, is defined by the global maximum of $\hbar\Omega_+^{(p)}$ in Eq. (49) with respect to $\mathbf{p}_f$, i.e., for $\mathbf{p}_f = \mathrm{sgn}(\mathbf{p}_i\cdot\mathbf{e}_z)e\mathbf{F}/\omega$ [where $\mathrm{sgn}(x) = \pm 1$ for $x \gtrless 0$],

$$\hbar\Omega_{\max}^{(p)} = \frac{p_i^2}{2m} + 2u_p + \frac{|e\mathbf{F}\cdot\mathbf{p}_i|}{m\omega} = \hbar\Omega_+^{(r)} - |E_0|, \quad (51)$$

where $\Omega_+^{(r)}$ is the upper boundary of the plateau in the radiative attachment or recombination spectrum (cf. Eq. (61) and Ref. [19]).

For a strong low-frequency field $\mathbf{F}(t)$, the number n of exchanged laser photons is large, so that the process of laser-assisted BrS can be described classically. In order to obtain the classical limit of the quantum result, (50), we perform the following transformations:

(i) For the Bessel function $J_n(\rho)$ in Eq. (50) we use its asymptotic expression for $|\rho| > |n| \gg 1$ [20],

$$J_n^2(\rho) \approx \frac{2\cos^2\phi}{\pi\sqrt{\rho^2 - n^2}}, \quad (52)$$

where $\phi = \sqrt{\rho^2 - n^2} - |n\arccos(n/\rho)| - \pi/4$. Owing to the rapid oscillations of the factor $\cos^2\phi$ in Eq. (52) as n varies, we set $\cos^2\phi = \langle\cos^2\phi\rangle = 1/2$.

(ii) We replace the summation over n in Eq. (50) by an integration over the final energies $p_f^2/(2m)$ in accordance with $dn \to p_f dp_f/(m\hbar\omega)$. We then use Eq. (46), which determines the dependence of the kinetic momenta $\mathbf{P}_{i,f}(t_0) = \mathbf{p}_{i,f} + (e/\omega)\mathbf{F}\sin\omega t_0$ on the final momentum $\mathbf{p}_f$ through the function $\sin\omega t_0 = n(\mathbf{p}_f)/\rho(\mathbf{p}_f)$. As a result we obtain

$$\frac{d\sigma^{(p)}}{d\Omega} = \frac{\omega}{\pi p_i}\int d\mathbf{p}_f\frac{P_i}{P_f}\frac{d^2\sigma^{(0)}/(d\Omega d\Omega_{\mathbf{P}_f})}{|e\mathbf{F}(t_0)\cdot(\mathbf{p}_i - \mathbf{p}_f)|}. \quad (53)$$

(iii) In Eq. (53) we now change the integration variables as follows: $\mathbf{p}_f \to \mathbf{P}_f$ and $|\mathbf{P}_f| \to t_0$. Using the relation

$$\mathbf{P}_f = \mathbf{p}_f + \mathbf{e}_z\frac{p_f^2 - p_i^2 + 2m\hbar\Omega}{2\mathbf{e}_z\cdot(\mathbf{p}_i - \mathbf{p}_f)},$$

we obtain, for the differential momentum space volume $d\mathbf{P}_f = P_f^2 dP_f d\Omega_{\mathbf{P}_f}$,

$$d\mathbf{P}_f = \left|\frac{\mathbf{e}_z\cdot\mathbf{P}_i}{\mathbf{e}_z\cdot(\mathbf{p}_i-\mathbf{p}_f)}\right| d\mathbf{p}_f.$$

We now express the differential dP_f in terms of dt_0, using the relation $dP_f = |\partial P_f/\partial t_0|dt_0 = (|\mathbf{P}_i\cdot e\mathbf{F}(t_0)|/P_f)dt_0$, where the latter equality is obtained using Eq. (47). It follows from Eq. (46) that two different values of t_0 (lying on different half-periods of the laser field) give the same values for the kinetic momenta $\mathbf{P}_{i,f}(t_0)$. Thus, the integration over time t_0 can be extended over the interval $0 \le t_0 \le T$, introducing the additional factor 1/2.

Finally, integrating over the angular variables $d\Omega_{\mathbf{P}_f}$, we obtain, for the BrS cross section,

$$\frac{d\sigma^{(\mathrm{cl})}(\mathbf{p}_i,\Omega)}{d\Omega} = \frac{1}{T}\int_0^T dt\,\frac{P_i(t)}{p_i}\frac{d\sigma^{(0)}(\mathbf{P}_i(t),\Omega)}{d\Omega}, \tag{54}$$

where $d\sigma^{(0)}(\mathbf{p},\Omega)/d\Omega = \int d\Omega_{\mathbf{p}'}d\sigma^{(0)}(\mathbf{p},\mathbf{p}')/d\Omega d\Omega_{\mathbf{p}'}$ is the field-free BrS spectral density. Equation (54) has a simple physical meaning: it describes the time-averaged BrS cross section over a period of the laser field in which the ratio $P_i(t)/p_i$ gives the time dependence of the incident electron flux.

B. Low-frequency results for LARA or LARR

The LARA or LARR amplitude for an initial scattering state in the Kroll-Watson approximation, $\Phi_{\mathbf{p}}^{(\mathrm{KW})}$ [cf. Eq. (42)], and a field-free final bound state, φ_{E_0}, is

$$\widetilde{\mathbf{d}}_\mu(\mathbf{p}) \approx \frac{1}{T}\int_0^T dt\, e^{i\mu\omega t + iS_{\mathbf{p}}(t)/\hbar}\widetilde{\mathbf{d}}^{(0)}(\mathbf{P}(t)), \tag{55}$$

where $\widetilde{\mathbf{d}}^{(0)}(\mathbf{P}(t)) = \langle\varphi_{E_0}|\mathbf{d}|\varphi_{\mathbf{P}(t)}\rangle$ is the field-free amplitude for electron radiative attachment or recombination with the initial momentum replaced by the laser-modified momentum $\mathbf{P}(t)$. Under the assumption $p_\parallel > |e|F/\omega$ (where $p_\parallel = \mathbf{p}\cdot\mathbf{e}_z > 0$), the saddle point equation $\mu\hbar\omega - \partial S_{\mathbf{p}}(t)/\partial t = 0$, or

$$\hbar\Omega_\mu = \frac{\mathbf{P}^2(t)}{2m} + |E_0|, \tag{56}$$

has only two solutions [21,22], $t = t_{1,2}$, such that $\mathbf{P}(t_1) = \mathbf{P}(t_2) \equiv \mathbf{P}$, where

$$\mathbf{P} = \mathbf{p}_\perp + \mathbf{e}_z\sqrt{2m(\hbar\Omega_\mu - |E_0|) - p_\perp^2} \tag{57}$$

and $\mathbf{p}_\perp = \mathbf{p} - \mathbf{e}_z p_\parallel$. By means of a saddle point analysis [similar to that used to derive Eq. (45)], we obtain for $\widetilde{\mathbf{d}}_\mu$ the low-frequency result

$$\widetilde{\mathbf{d}}_\mu(\mathbf{p}) = c_\mu(\mathbf{p})\,\widetilde{\mathbf{d}}^{(0)}(\mathbf{P}), \tag{58}$$

where $c_\mu(\mathbf{p})$ is the Fourier coefficient of the Volkov wave $\chi_{\mathbf{p}}(0,t)$ at $\mathbf{r} = 0$, expressed in terms of the generalized Bessel function $[J_\mu(u,v) = \sum_{k=-\infty}^{\infty} J_{\mu-2k}(u)J_k(v)]$:

$$c_\mu(\mathbf{p}) = i^{-\mu}J_\mu\left(\frac{e\mathbf{F}\cdot\mathbf{p}}{m\hbar\omega^2},\frac{u_p}{2\hbar\omega}\right). \tag{59}$$

Substituting result (58) into Eq. (36), we obtain, for the LARA or LARR cross section,

$$\widetilde{\sigma}_\mu(\mathbf{p}) = \frac{|\mathbf{P}|}{p}J_\mu^2\left(\frac{e\mathbf{F}\cdot\mathbf{p}}{m\hbar\omega^2},\frac{u_p}{2\hbar\omega}\right)\widetilde{\sigma}^{(0)}(|\mathbf{P}|), \tag{60}$$

where the field-free cross section $\widetilde{\sigma}^{(0)}(|\mathbf{P}|)$ involves the absolute value of the instantaneous kinetic momentum, $|\mathbf{P}| = \sqrt{2m(\hbar\Omega_\mu - |E_0|)}$.

The saddle point equation, (56), has real solutions only for the interval $\Omega_-^{(r)} < \Omega_\mu < \Omega_+^{(r)}$ of spontaneous photon frequencies. Within this interval, the average value of the cross section $\widetilde{\sigma}_\mu$ depends weakly on Ω_μ, forming a plateau in the LARA or LARR spectrum [21–23]. Under the condition $p_\parallel > |e|F/\omega$, the lower ($\Omega_-^{(r)}$) and upper ($\Omega_+^{(r)}$) boundaries of this plateau are

$$\hbar\Omega_\pm^{(r)} = |E_0| + \frac{p^2}{2m} + 2u_p \pm \frac{|e\mathbf{F}\cdot\mathbf{p}|}{m\omega}. \tag{61}$$

Analysis of Eqs. (57) and (58) shows that for nonzero $\mathbf{p}_\perp$ the angular distribution of the spontaneous radiation changes with variation of Ω_μ: for high Ω_μ the direction of the dipole moment $\widetilde{\mathbf{d}}_\mu(\mathbf{p})$ is predominantly determined by the laser polarization $\mathbf{e}_z$. Indeed, as shown by Eq. (58), the direction of the vector $\widetilde{\mathbf{d}}_\mu(\mathbf{p})$ is determined by the field-free dipole moment $\widetilde{\mathbf{d}}^{(0)}(\mathbf{P})$, which in turn is directed along the instantaneous kinetic momentum $\mathbf{P}$. It then follows from Eq. (57) that with increasing Ω_μ the angle between $\mathbf{P}$ and $\mathbf{e}_z$ decreases.

The analytic results, (58) and (60), generalize previous results in Ref. [19], where $\widetilde{\sigma}_\mu$ was expressed in terms of an Airy function, describing the LARA or LARR spectrum only in the region of the upper cutoff.

C. The ionization and detachment amplitude within the Keldysh theory

For the ν-photon above-threshold detachment amplitude $A_\nu^{(\mathrm{det})}$, which is involved in the resonant part of the BrS cross section [cf. Eq. (35)], an approximate result can be found by replacing the QQES wave function $\Phi_\varepsilon(\mathbf{r},t)$ in Eq. (29) by the field-free bound state $\varphi_{E_0}(\mathbf{r})$. Such a substitution corresponds to the well-known Keldysh approximation [24] (see also the review [25] and references therein).

In terms of the Fourier coefficients $c_\nu(\mathbf{p})$ of the Volkov wave $\chi_{\mathbf{p}}(\mathbf{r},t)$ [cf. Eq. (59)], the amplitude $A_\nu^{(\mathrm{det})}$ for a bound s state is expressed as [7]

$$A_\nu^{(\mathrm{det})}(\mathbf{p}_\nu) = \frac{C_\kappa}{\sqrt{4\pi}}c_{-\nu}^*(\mathbf{p}_\nu), \tag{62}$$

where C_κ is the asymptotic coefficient of the wave function $\varphi_{E_0}(\mathbf{r})$ as $r \to \infty$.

IV. ELECTRON-ATOM BREMSSTRAHLUNG WITHIN TDER THEORY

A. The exact BrS dipole matrix element

To obtain numerical results for laser-assisted BrS, we use TDER theory to describe the continuum field-dressed state ($\Phi_{\mathbf{p}}$) of an active electron [26,27], scattering from a short-range atomic potential $U(r)$ that vanishes for $r \gtrsim r_c$.

The TDER theory assumes that the potential $U(r)$ supports a single weakly bound state (a negative-ion state) with energy $E_0 = -\hbar^2\kappa^2/(2m)$ ($\kappa r_c \ll 1$) and angular momentum l. The electron-atom interaction is described by the l-wave scattering phase $\delta_l(p)$ that is parameterized by the scattering length a_l and the effective range r_l, which are parameters of the problem

$$k^{2l+1}\cot\delta_l(p) = -a_l^{-1} + r_l k^2/2, \quad k = p/\hbar.$$

For simplicity we consider the case of a bound s state ($l = 0$), so that only the phase shift $\delta_0(p)$ is nonzero. For this case, the TDER wave function $\Phi_{\mathbf{p}}(\mathbf{r},t)$ is expressed in terms of a one-dimensional integral [26],

$$\Phi_{\mathbf{p}}(\mathbf{r},t) = \chi_{\mathbf{p}}(\mathbf{r},t) - \frac{2\pi\hbar^2}{m\kappa}\int_{-\infty}^{t} dt' e^{i\epsilon(t-t')/\hbar} \times G(\mathbf{r},t;0,t')f_{\mathbf{p}}(t'), \tag{63}$$

where the incident wave $\chi_{\mathbf{p}}(\mathbf{r},t)$ is given by Eq. (14), $G(\mathbf{r},t;\mathbf{r}',t')$ is the nonstationary retarded Green's function of a free electron in a laser field $\mathbf{F}(t)$ [the Volkov Green's function; cf. Eq. (A5)], and $f_{\mathbf{p}}(t)$ is the time-periodic function,

$$f_{\mathbf{p}}(t) = \sum_{k=-\infty}^{\infty} f_k(\mathbf{p})e^{-ik\omega t}. \tag{64}$$

The Fourier coefficients $f_k(\mathbf{p})$ in Eq. (64) satisfy the system of inhomogeneous linear algebraic equations [7]

$$\sum_{k'} \mathcal{M}_{k,k'}(\epsilon) f_{k'}(\mathbf{p}) = c_k(\mathbf{p}), \tag{65}$$

where $c_k(\mathbf{p})$ is given by Eq. (59) and the matrix elements $\mathcal{M}_{k,k'}(\epsilon)$ have the following form:

$$\mathcal{M}_{k,k'}(\epsilon) = [\kappa\mathcal{A}(\tilde{p}_k)]^{-1}\delta_{k,k'} - \hat{\mathcal{M}}_{k,k'}(\epsilon), \tag{66}$$

$$\mathcal{A}(\tilde{p}_k) = \frac{\hbar}{\tilde{p}_k[\cot\delta_0(\tilde{p}_k) - i]}, \quad \tilde{p}_k = \sqrt{2m(\epsilon + k\hbar\omega)}, \tag{67}$$

$$\hat{\mathcal{M}}_{k,k'}(\epsilon) = \sqrt{\frac{i^{k-k'}m\omega}{4\pi i\hbar\kappa^2}}\int_0^{\infty}\frac{d\phi}{\phi^{3/2}}\, e^{i[2\epsilon/(\hbar\omega)+(k+k')]\phi} \times [e^{i\lambda(\phi)}J_{(k-k')/2}(z(\phi)) - \delta_{k,k'}], \tag{68}$$

$$\lambda(\phi) = \frac{2u_p}{\hbar\omega}\left(\frac{\sin^2\phi}{\phi} - \phi\right),$$

$$z(\phi) = \frac{u_p}{\hbar\omega}\left(\sin 2\phi - \frac{2\sin^2\phi}{\phi}\right).$$

The exact TDER result, (63), for the scattering state $\Phi_{\mathbf{p}}(\mathbf{r},t)$ contains the information on electron-atom dynamics through the function $f_{\mathbf{p}}(t)$, which is therefore the key object of TDER theory. Moreover, Eqs. (65) and (66) show that only diagonal matrix elements $\mathcal{M}_{k,k'}$ contain this information [i.e., the field-free elastic s-wave scattering amplitude $\mathcal{A}(\tilde{p}_k)$ for a "momentum" $\tilde{p}_k$, which is imaginary for closed channels with $\epsilon + k\hbar\omega < 0$]. In contrast, the nondiagonal elements ($k \neq k'$) depend only on the incident electron energy $p^2/(2m)$ and the laser parameters. [Note that in the low-frequency approximation, the function $f_{\mathbf{p}}(t)$ itself is proportional to the amplitude $\mathcal{A}$; cf. Eq. (91).] The matrix elements $\hat{\mathcal{M}}_{k,k'}$ in Eq. (68) are nonzero only if the difference $k - k'$ is even, so that equations for $f_k(\mathbf{p})$ with even and odd k are not coupled. From the explicit form, (68), of $\hat{\mathcal{M}}_{k,k'}(\epsilon)$ follow the symmetry relations

$$\mathcal{M}_{k,k'}(\epsilon) = \mathcal{M}_{k',k}(\epsilon), \tag{69}$$

$$\mathcal{M}_{k,k'}(\epsilon + \mu\hbar\omega) = \mathcal{M}_{k+\mu,k'+\mu}(\epsilon). \tag{70}$$

The TDER result for the dipole moment $\mathbf{d}_n$ follows after substituting the wave functions of the initial ($\Phi_{\mathbf{p}_i}$) and final ($\Phi_{\mathbf{p}_f}$) QESs in the form of (63) into Eq. (7),

$$\mathbf{d}_n(\mathbf{p}_i,\mathbf{p}_f) = \frac{1}{T}\int_0^T dt e^{in\omega t}\big(\langle\chi_{\mathbf{p}_f}(t)|\mathbf{d}|\chi_{\mathbf{p}_i}(t)\rangle + \langle\chi_{\mathbf{p}_f}(t)|\mathbf{d}|\Phi^{(+)}_{\mathbf{p}_i}(t)\rangle + \langle\Phi^{(-)}_{\mathbf{p}_f}(t)|\mathbf{d}|\chi_{\mathbf{p}_i}(t)\rangle + \langle\Phi^{(-)}_{\mathbf{p}_f}(t)|\mathbf{d}|\Phi^{(+)}_{\mathbf{p}_i}(t)\rangle\big), \tag{71}$$

where the functions $\Phi^{(+)}_{\mathbf{p}} = \Phi_{\mathbf{p}} - \chi_{\mathbf{p}}$ and $\Phi^{(-)}_{\mathbf{p}} = \Phi^{\mathcal{T}}_{\mathbf{p}} - \chi_{\mathbf{p}}$ describe outgoing and ingoing waves respectively, which are expressed in terms of retarded $G^{(+)} \equiv G$ and advanced $G^{(-)}$ Volkov Green's functions [cf. Eq. (A5)]:

$$\Phi^{(+)}_{\mathbf{p}}(\mathbf{r},t) = -\frac{2\pi\hbar^2}{m\kappa}\int_{-\infty}^{t} dt' e^{i\epsilon(t-t')/\hbar} \times G^{(+)}(\mathbf{r},t;0,t')f_{\mathbf{p}}(t'), \tag{72}$$

$$\Phi^{(-)}_{\mathbf{p}}(\mathbf{r},t) = -\frac{2\pi\hbar^2}{m\kappa}\int_{t}^{\infty} dt' e^{i\epsilon(t-t')/\hbar} \times G^{(-)}(\mathbf{r},t;0,t')f^{\mathcal{T}}_{\mathbf{p}}(t'). \tag{73}$$

Note that inversion of time does not change the Volkov wave function: $\chi^{\mathcal{T}}_{\mathbf{p}} = \chi_{\mathbf{p}}$.

Details of the evaluation of the spatial and temporal integrals in Eq. (71) are presented in the Appendix. The result for the BrS dipole matrix element is

$$\mathbf{d}_n = \mathbf{d}^{(0)}_n + \hat{\mathbf{p}}_i\chi_1 + \hat{\mathbf{p}}_f\chi_2 + \mathbf{e}_z\chi_3, \tag{74}$$

where $\hat{\mathbf{p}}_i \equiv \mathbf{p}_i/p_i$, $\hat{\mathbf{p}}_f \equiv \mathbf{p}_f/p_f$,

$$\mathbf{d}^{(0)}_n = 4(\pi\hbar)^3\frac{e^2\mathbf{F}}{m\omega^2}\delta(\mathbf{p}_i - \mathbf{p}_f)\delta_{n,1}, \tag{75}$$

$$\chi_1 = 2iC\frac{\omega p_i}{eF}\mathcal{L}^{(1)}_n, \; \chi_2 = -2iC\frac{\omega p_f}{eF}\mathcal{L}^{(2)}_n, \tag{76}$$

$$\chi_3 = C\left(\sum_{s=\pm1}\frac{\mathcal{L}^{(1)}_{n+s} - \mathcal{L}^{(2)}_{n+s}}{\omega/\Omega + s} + \mathcal{K}_n\right), \tag{77}$$

$$C = \frac{\pi\hbar e^2 F}{\kappa m^2\Omega^2\omega},$$

$$\mathcal{L}^{(1)}_n = \sum_k c_{k+n}(\mathbf{p}_i)f_k(-\mathbf{p}_f), \tag{78}$$

$$\mathcal{L}^{(2)}_n = \sum_k c_{k-n}(-\mathbf{p}_f)f_k(\mathbf{p}_i), \tag{79}$$

$$\mathcal{K}_n = \sum_{k,k'} f_k(\mathbf{p}_i) f_{k-n+1+2k'}(-\mathbf{p}_f) W_{k,k'}, \tag{80}$$

$$W_{k,k'} = \frac{i^{k'}}{\kappa}\sqrt{\frac{m\omega}{\pi i\hbar}}\int_0^\infty \frac{d\phi}{\phi^{3/2}} e^{i[(2\epsilon_i/\hbar-\Omega)/\omega+2k+2k'+1]\phi} \times e^{i\lambda(\phi)}[j_-(\phi)J_{k'}(z(\phi)) - i j_+(\phi)J_{k'+1}(z(\phi))],$$

$$j_\pm(\phi) = \frac{1}{\phi}\sin\phi\sin\frac{\Omega\phi}{\omega} - \frac{\Omega}{\Omega\pm\omega}\sin\frac{(\Omega\pm\omega)\phi}{\omega}. \tag{81}$$

The term $\mathbf{d}_n^{(0)}$ in Eq. (74) describes spontaneous emission of a photon with $\Omega = \omega$ and corresponds to Thomson scattering of the laser radiation from a free electron. In what follows, we omit this term from our considerations. The term $\mathcal{K}_n$ in Eq. (77) originates from the last matrix element in Eq. (71), $\langle\Phi_{\mathbf{p}_f}^{(-)}|\mathbf{d}|\Phi_{\mathbf{p}_i}^{(+)}\rangle$, involving two Volkov Green's functions [see also Eqs. (A11) and (A12)]. Accordingly, the explicit form, (80), for $\mathcal{K}_n$ involves products of the Fourier coefficients of $f_{\mathbf{p}}(t)$, and thus this term describes rescattering effects in the laser-assisted BrS process (cf. Ref. [27]).

The exact TDER result for the dipole moment $\mathbf{d}_n$, given by Eq. (74), represents a bounded function of Ω over the entire BrS spectrum. To confirm this statement, let us consider the first term in Eq. (77) for χ_3 for $\Omega = \omega$ and $s = -1$. Although the denominator $(\omega/\Omega - 1)$ tends to 0 as $\Omega \to \omega$, the corresponding numerator Λ is also equal to 0:

$$\Lambda = \left(\mathcal{L}_{n-1}^{(1)} - \mathcal{L}_{n-1}^{(2)}\right)\big|_{\Omega=\omega} = 0. \tag{82}$$

Indeed, the solution of Eqs. (65) for $f_k(\mathbf{p})$ can be written in terms of the inverse matrix $\mathcal{M}^{-1}$ of the matrix $\mathcal{M}$:

$$f_k(\mathbf{p}) = \sum_{k'}[\mathcal{M}^{-1}]_{k,k'}(\epsilon)c_{k'}(\mathbf{p}). \tag{83}$$

Substituting $f_k(\mathbf{p}_i)$ and $f_k(\mathbf{p}_f)$ in the form of (83) into Eqs. (78) and (79), and taking into account the symmetry relations (69) and (70) and the relation $\epsilon_f = \epsilon_i + (n-1)\hbar\omega$, we obtain

$$\Lambda = \sum_{k,k'}\{c_{k+n-1}(\mathbf{p}_i)[\mathcal{M}^{-1}]_{k+n-1,k'+n-1}(\epsilon_i)c_{k'}(-\mathbf{p}_f) - c_{k-n+1}(-\mathbf{p}_f)[\mathcal{M}^{-1}]_{k',k}(\epsilon_i)c_{k'}(\mathbf{p}_i)\}. \tag{84}$$

Finally, changing the summation indices $k \to k' - n + 1$ and $k' \to k - n + 1$ in the first term in Eq. (84), we obtain result (82).

B. Low-frequency approximation for resonant BrS within TDER theory

The low-frequency results for the key ingredients [$\mathbf{d}_n^{(p)}$, $\widetilde{\mathbf{d}}_\mu$, and $A_\nu^{(\mathrm{det})}$] of the resonant BrS process obtained in Sec. III take closed analytic forms within TDER theory owing to its analytic expressions for the field-free atomic factors. The latter can be found using the following asymptotic ($r > r_c$) expressions for the field-free bound state, $\varphi_{E_0}(\mathbf{r})$, and the continuum scattering state, $\varphi_{\mathbf{p}}(\mathbf{r})$, of the active electron:

$$\varphi_{E_0}(\mathbf{r}) = \frac{C_\kappa}{\sqrt{4\pi}}\frac{e^{-\kappa r}}{r}, \tag{85}$$

$$\varphi_{\mathbf{p}}(\mathbf{r}) = e^{i\mathbf{p}\mathbf{r}/\hbar} + \mathcal{A}(p)\frac{e^{ipr/\hbar}}{r}, \tag{86}$$

where $C_\kappa = \sqrt{2\kappa/(1-r_0\kappa)}$ is the asymptotic coefficient expressed in terms of r_0 and κ, and $\mathcal{A}(p)$ is the elastic s-wave scattering amplitude, given by Eq. (67). Using Eqs. (85) and (86) to evaluate the dipole matrix elements for field-free BrS [i.e., $\mathbf{d}^{(0)}(\mathbf{p},\mathbf{p}')$ on the right-hand side of Eq. (45)] and for radiative attachment [i.e., $\widetilde{\mathbf{d}}^{(0)}(\mathbf{p})$ on the right of Eq. (58)], we obtain

$$\mathbf{d}^{(0)}(\mathbf{p},\mathbf{p}') = \frac{2\pi i e\hbar}{m^2\Omega^2}[\mathbf{p}\mathcal{A}(p') - \mathbf{p}'\mathcal{A}(p)], \tag{87}$$

$$\widetilde{\mathbf{d}}^{(0)}(\mathbf{p}) = \frac{4i\sqrt{\pi}C_\kappa e\mathbf{p}}{\hbar[\kappa^2 + (p/\hbar)^2]^2}. \tag{88}$$

The low-frequency result, (45) [with the field-free atomic factor $\mathbf{d}^{(0)}$ defined by Eq. (87)], for the potential part of the BrS dipole moment can be derived directly from the exact TDER results presented in Sec. IV A. To show this we note that the terms $\mathcal{L}_n^{(1,2)}$, which are involved in $\mathbf{d}_n$ through the "susceptibilities" $\chi_{1,2,3}$ [cf. Eqs. (74) and (77)] and which are defined by Eqs. (78) and (79), can be defined alternatively by

$$\mathcal{L}_n^{(1)} = \frac{1}{T}\int_0^T dt e^{in\omega t + iS_{\mathbf{p}_i}(t)/\hbar} f_{-\mathbf{p}_f}(-t), \tag{89}$$

$$\mathcal{L}_n^{(2)} = \frac{1}{T}\int_0^T dt e^{in\omega t + iS_{-\mathbf{p}_f}(-t)/\hbar} f_{\mathbf{p}_i}(t), \tag{90}$$

where the function $f_{\mathbf{p}}(t)$ in the low-frequency (nonresonant) approximation can be written as [28]

$$f_{\mathbf{p}}(t) \approx \kappa\mathcal{A}(P(t))e^{iS_{\mathbf{p}}(t)/\hbar}, \tag{91}$$

which represents the iterative solution of Eqs. (65) in the lowest order of the parameter $\hbar\omega/u_p$. Using Eq. (91) for $f_{\mathbf{p}_i}(t)$ and $f_{-\mathbf{p}_f}(-t)$ [noting that from the explicit form (15) for $S_{\mathbf{p}}(t)$, it follows that $S_{-\mathbf{p}}(-t) = -S_{\mathbf{p}}(t)$], the integrals in Eqs. (89) and (90) for $\mathcal{L}_n^{(1,2)}$ in the low-frequency approximation can be evaluated using the saddle point method, which gives

$$\mathcal{L}_n^{(1)} = i^n\kappa\mathcal{A}(P_f(t_0))J_n(\rho), \tag{92}$$

$$\mathcal{L}_n^{(2)} = i^n\kappa\mathcal{A}(P_i(t_0))J_n(\rho), \tag{93}$$

$$\mathcal{L}_{n+1}^{(k)} - \mathcal{L}_{n-1}^{(k)} = 2i\mathcal{L}_n^{(k)}\sin\omega t_0, \quad k = 1,2, \tag{94}$$

where ρ is defined in Eq. (44), and t_0 is the solution of the saddle point equation, (46). Furthermore, in the low-frequency limit, one can neglect the rescattering term $\mathcal{K}_n$ in Eq. (77) in comparison with $\mathcal{L}_n^{(1,2)}$. To see this, we note that (i) in accordance with Eq. (91), the coefficients f_k are of the order of the elastic scattering amplitude $\mathcal{A}$, $f_k \sim \kappa\mathcal{A}$; (ii) it follows from the saddle point analysis of the integral in Eq. (81) that the factors $W_{k,k'}$ are of the order of the inverse of the amplitude α_0 of free-electron oscillations in

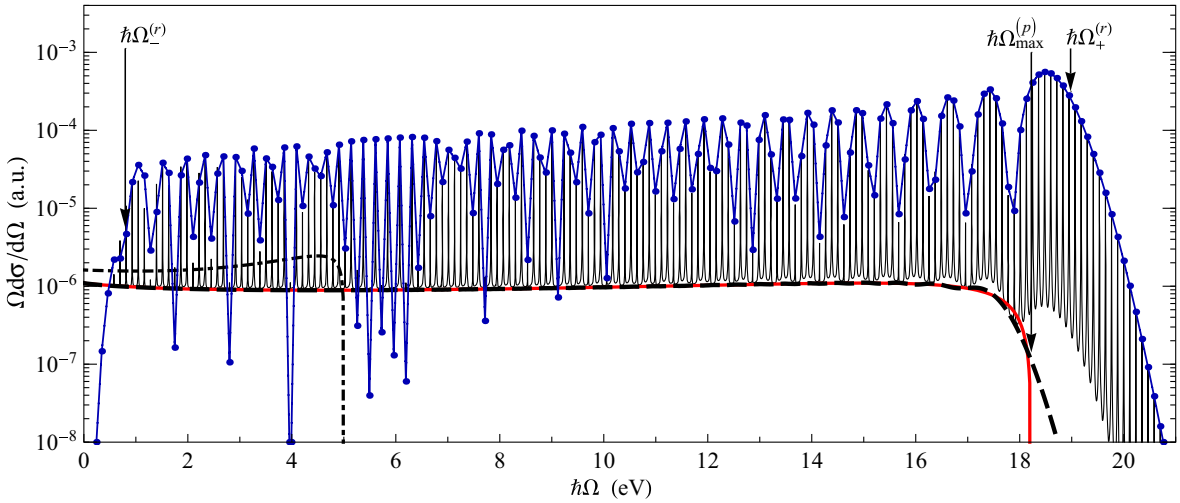

FIG. 2. (Color online) Spectral density, (10), of laser-assisted e-H BrS in a CO_2 laser field with $\hbar\omega = 0.117$ eV ($\lambda = 10.6$ μm) and intensity $I = 2 \times 10^{11}$ W/cm^2. The incident electron energy is $p_i^2/(2m) = 5$ eV and $\mathbf{p}_i \| \mathbf{e}_z$. Thin solid (black) line—exact TDER result; dashed (black) line—low-frequency result, (50); thick solid (red) line—classical limit result, (54); filled circles connected by lines (blue)—scaled cross section for radiative e-H attachment, given by Eq. (95); dot-dashed (black) line—field-free BrS spectrum. Vertical arrows indicate the lower ($\Omega_-^{(r)}$) and upper ($\Omega_+^{(r)}$) cutoffs [cf. Eq. (61)] of the LARA spectrum plateau as well as the plateau cutoff $\Omega_{\max}^{(p)}$ [cf. Eq. (51)] for the nonresonant laser-assisted BrS spectrum; note that $\hbar(\Omega_+^{(r)} - \Omega_{\max}^{(p)}) = |E_0|$.

the field $\mathbf{F}(t)$, $W_{k,k'} \sim (\kappa\alpha_0)^{-1}$, where $\alpha_0 = |e|F/(m\omega^2)$; and (iii) the field-free atomic scattering amplitude is of the order of the range of the atomic potential and hence much lower than the amplitude α_0 in a low-frequency laser field, i.e., $|\mathcal{A}| \ll \alpha_0$. Finally, substituting Eqs. (92)–(94) into Eqs. (76) and (77), we obtain result (45), where the field-free dipole moment $\mathbf{d}^{(0)}$ is given by the TDER result, (87). We note that the omitted terms $\sim\mathcal{K}_n$ and higher order corrections (in the parameter $\hbar\omega/u_p$) to $f_{\mathbf{p}}(t)$ describe rescattering effects in the BrS process [28].

C. Numerical results for the electron-atom BrS spectral density

The key features of the laser-assisted BrS spectral density [defined in Eq. (10)] are shown in Fig. 2. The exact TDER results [obtained using Eq. (74) for $\mathbf{d}_n(\mathbf{p}_i, \mathbf{p}_f)$ in Eq. (10)] for e-H BrS in a CO_2 laser field with intensity $I = 2 \times 10^{11}$ W/cm^2 and photon energy $\hbar\omega = 0.117$ eV are compared with the field-free BrS spectrum, with the low-frequency analytic result, (50), and with its classical limit, (54). The TDER parameters employed are (cf., e.g., [29]) $|E_0| = 0.755$ eV, $C_\kappa = 2.304$, $a_0 = 6.16a_B$, and $r_0 = 2.64a_B$, where a_B is the Bohr radius. Figure 2 exhibits several key features, as follows.

(i) For resonant frequencies $\Omega = \Omega_\mu$ [where Ω_μ is defined in Eq. (11) and where $\Omega_{\mu+1} - \Omega_\mu = \omega$], the BrS spectral density has resonant peaks at which $d\sigma(\Omega_\mu)/d\Omega$ increases by up to three orders of magnitude compared with the nonresonant case. Remarkably, the spectral density at the resonant frequencies exceeds the value of the corresponding field-free BrS density. (Usually in a laser field the nonresonant BrS spectral density is lower than its field-free counterpart.)

(ii) The BrS spectrum at the resonant frequencies replicates the LARA spectrum, i.e., the spectral density $d\sigma(\Omega_\mu)/d\Omega$ at the resonant frequency Ω_μ may be approximated by

$$\frac{d\sigma(\Omega_\mu)}{d\Omega} \approx \frac{d\sigma^{(\mu)}(\Omega)}{d\Omega}\bigg|_{\Omega=\Omega_\mu} = \frac{2\hbar}{\pi\Gamma}\,\widetilde{\sigma}_\mu, \tag{95}$$

where the first approximate equality follows from neglect of the nonresonant part of the BrS spectral density and the second equality follows from Eq. (39) upon substituting $\delta = 0$ there.

The resonant peaks in the BrS spectrum form a plateau-like structure with upper and lower cutoffs at $\Omega = \Omega_\pm^{(r)}$, where $\Omega_\pm^{(r)}$ corresponds to the cutoffs of the LARA spectrum, defined in Eq. (61). The oscillatory behavior of $d\sigma(\Omega_\mu)/d\Omega$ as a function of Ω_μ originates from that of the generalized Bessel function in the analytic formula, (60), for the LARA cross section. For low spontaneous photon energies (such that $\Omega < \Omega_-^{(r)}$), the resonant peaks decrease significantly as Ω decreases.

(iii) For nonresonant Ω, the BrS spectrum is well described both by the low-frequency approximation result, (50), and by its classical limit, (54), up to the plateau cutoff of the nonresonant BrS spectrum at $\Omega_{\max}^{(p)}$, which is defined in Eq. (51). For $\Omega > \Omega_{\max}^{(p)}$ the exact BrS spectrum at nonresonant Ω is much larger than the low-frequency and classical results due to overlaps of the wings of adjacent resonant peaks. In order to estimate the cross section $d\sigma/d\Omega$ between these peaks (i.e., at $\Omega = \Omega_\mu + \omega/2$), we add to the potential BrS cross section the contributions from the wings of both adjacent resonances evaluated at this energy in accordance with Eq. (39):

$$\frac{d\sigma(\Omega_\mu + \omega/2)}{d\Omega} \approx \frac{d\sigma^{(p)}(\Omega_\mu + \omega/2)}{d\Omega} + \frac{2\Gamma}{\pi\hbar\omega^2}(\widetilde{\sigma}_\mu + \widetilde{\sigma}_{\mu+1}). \tag{96}$$

For $\Omega > \Omega_{\max}^{(p)}$ the nonresonant part $d\sigma^{(p)}/d\Omega$ of the BrS spectral density decreases rapidly. Comparing the on-resonance result, (95), with the off-resonance result, (96) (in which we ignore $d\sigma^{(p)}/d\Omega$), we find that the magnitude of the resonant enhancement of $d\sigma/d\Omega$ is governed by the factor $\Delta \simeq (\hbar\omega)^2/(2\Gamma^2)$, where $\Gamma = 2.2 \times 10^{-3}$ eV and $\Delta = 1.3 \times 10^3$ for laser parameters as in Fig. 2.

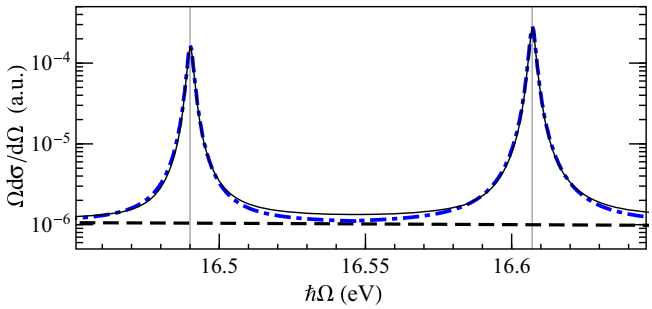

FIG. 3. (Color online) The same as Fig. 2, but for frequencies Ω in the vicinity of two adjacent resonances on an expanded energy scale. Thin solid (black) line—exact TDER result; dot-dashed (blue) line—Eqs. (34) and (35); dashed (black) line—low-frequency result, (48), for nonresonant BrS. The vertical lines indicate the two resonant frequencies Ω_μ.

In Fig. 3 we present resonant profiles for two adjacent resonances in the BrS cross section. The spectral density is evaluated using both the exact TDER equations and the general parametrization, (35). For the dipole moments $\mathbf{d}_n^{(p)}$ and $\widetilde{\mathbf{d}}_\mu$ and the amplitude $A_\nu^{(\mathrm{det})}$, all of which are involved in Eq. (35), as well as for the potential part of the BrS cross section in Eq. (34), we use the analytic formulas of the low-frequency approximation, discussed in Secs. III and IV B. As shown in Fig. 3, the analytic results are in excellent agreement with the exact TDER results for both resonant and nonresonant energies of the BrS photon.

For a deeper understanding of resonant phenomena in the BrS process, in the following we analyze the BrS spectral density obtained after integrating the doubly differential cross section over a finite interval of final electron energies, $E_f = p_f^2/(2m)$, and momentum directions, which are defined by the polar (θ_f) and azimuthal (φ_f) angles with respect to the laser polarization vector $\mathbf{e}_z$. The integrations over the angles φ_f and θ_f are over the intervals $[0,360^\circ]$ and $[\theta_f,\theta_f + 10^\circ]$, respectively (cf. Fig. 4).

In Fig. 5 we show the dependence of the resonant channel contribution to the BrS process on the final (scattered) electron state. One sees that resonant phenomena become less pronounced as the final electron energy E_f increases [cf. Figs. 5(a) and 5(b)]. This fact stems from the behavior of the detachment factor, i.e., the detachment rate $dR(\mathbf{p}_\nu)/d\Omega_{\mathbf{p}_\nu}$ in Eq. (35). Specifically, the energy interval 3 eV $< E_f <$ 4 eV in Fig. 5(a) belongs to the low-energy plateau in the above threshold detachment spectrum, which extends up to $\sim 2u_p$ ($u_p = 2.07$ eV for the parameters in Fig. 5) and is well described within the Keldysh approximation. The interval 4.5 eV $< E_f <$ 5.5 eV in Fig. 5(b) corresponds to the region beyond the Keldysh plateau cutoff, where $dR(\mathbf{p}_\nu)/d\Omega_{\mathbf{p}_\nu}$ decreases by several orders of magnitude and rescattering effects become significant (e.g., cf. Ref. [30]). The detachment factor $dR(\mathbf{p}_\nu)/d\Omega_{\mathbf{p}_\nu}$ is also responsible for a less pronounced manifestation of resonance effects in the BrS spectrum as $|\cos\theta_f|$ decreases [cf. Figs. 5(a) and 5(c)]: the laser field detaches the virtually captured electron predominantly along the laser polarization direction. For scattering at small angles $\theta_f \to 0$ the position of the upper cutoff $\hbar\Omega_+^{(p)}$ [cf. Eq. (49)] of the plateau in the nonresonant BrS spectrum is shifted to the region of low energies $\hbar\Omega$, so that for high energies $\hbar\Omega$ in Fig. 5(d) the BrS spectrum is dominated by the resonance structures.

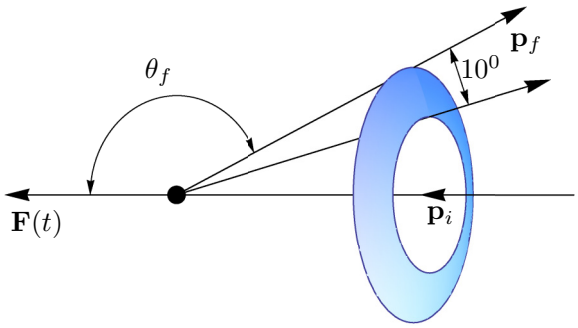

FIG. 4. (Color online) Geometry of the incident ($\mathbf{p}_i$) and final ($\mathbf{p}_f$) electron momenta and the laser electric field, $\mathbf{F}(t)$. The shaded (blue) area denotes the integration domain over the final electron directions.

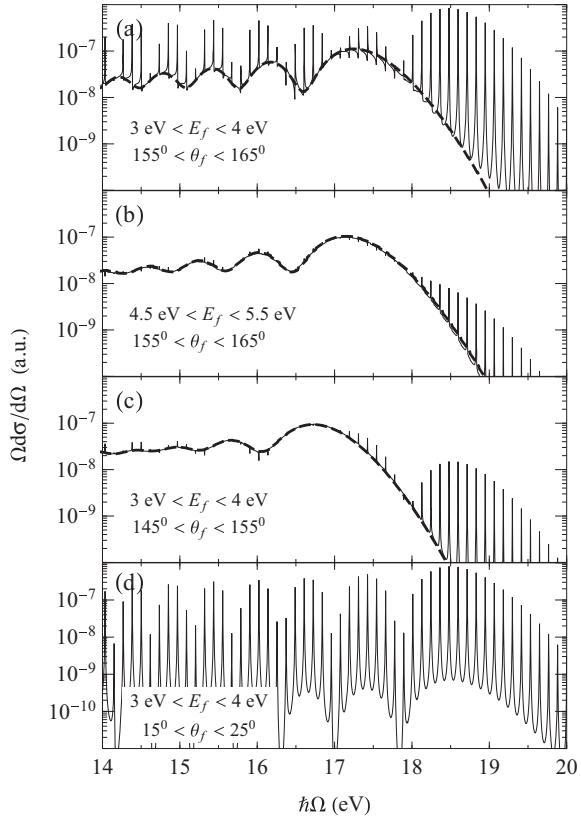

FIG. 5. e-H BrS spectral density integrated over different intervals of the final electron energies and directions (shown in each panel). The laser field parameters and initial electron energy are the same as in Fig. 2. Thin solid lines—exact TDER results; thick dashed lines—low-frequency result, (48), for nonresonant BrS.

These results show that the potential and resonant parts of the BrS cross section are comparable for backward electron scattering with low final energies ($\lesssim 2u_p$). In this case interference between the potential and the resonant BrS

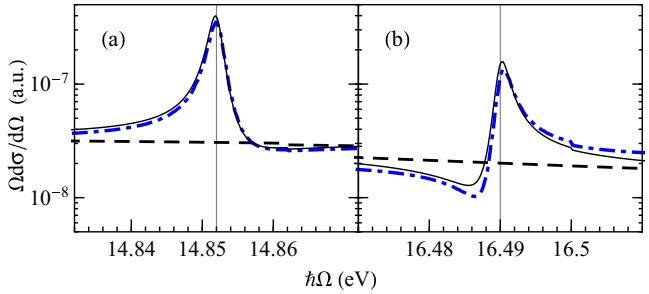

FIG. 6. (Color online) The same as Fig. 5, but for frequencies Ω in the vicinity of two particular resonances Ω_μ: (a) $\mu = 60$, $\Omega_{60} = 14.85$ eV and (b) $\mu = 74$, $\Omega_{74} = 16.49$ eV. The intervals of final electron energies and directions are 3.1 eV $< E_f <$ 4.3 eV, $155^\circ < \theta_f < 165^\circ$. Thin solid (black) line—exact TDER result; dot-dashed (blue) line—Eqs. (34) and (35); dashed (black) line—low-frequency result, (48), for nonresonant BrS. Vertical lines indicate the two resonant frequencies Ω_μ.

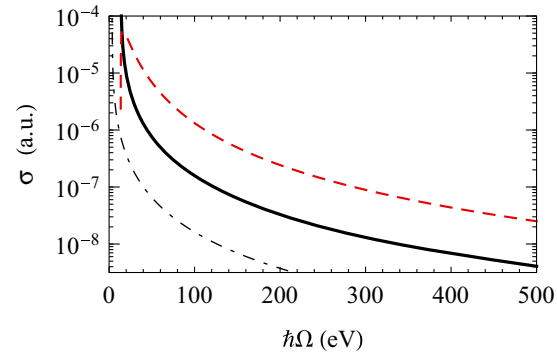

FIG. 7. (Color online) Field-free electron-proton radiative recombination cross sections. Thick solid line, exact result for recombination into the ground $1s$ state of the H atom; dashed (red) line, Born approximation result for recombination into the $1s$ state of the H atom; dot-dashed line, exact result for recombination into the $2s$ state of the H atom.

amplitudes leads to asymmetric resonant profiles in the BrS spectral density, as shown in Fig. 6, where $d\sigma/d\Omega$ is obtained after integration of the BrS doubly differential cross section over the domain 3.1 eV $< E_f <$ 4.3 eV, $155^\circ < \theta_f < 165^\circ$. The exact TDER results are in good agreement with the parametrization of resonant BrS given in Eqs. (34) and (35). Note that pronounced asymmetries in the resonance profiles disappear at high energies $\hbar\Omega$ when one integrates over all final electron momenta owing to the dominance of the resonant cross section over that of the nonresonant cross section (cf. Fig. 3).

V. ESTIMATES OF LASER-ASSISTED BREMSSTRAHLUNG IN ELECTRON SCATTERING FROM A COULOMB POTENTIAL

The analytic results for the BrS spectral density that we have obtained for a short-range potential may be extended to the case of a Coulomb potential by replacing terms dependent on the short-range potential by terms appropriate for a Coulomb potential. Note that we are not able to discuss resonance profiles in a Coulomb potential because that involves knowing the relative phases between resonant and nonresonant amplitudes in order to obtain the parameter q in Eq. (38). In the following analysis we assume that the laser parameters and the incident electron energy are such that (i) the resonant peak widths are significantly smaller than the distance between neighboring peaks (i.e., we assume $\Gamma \ll \hbar\omega$), and (ii) the potential (nonresonant) part of the BrS amplitude is negligible in comparison with the resonant one in the vicinity of the resonant frequencies $\Omega \approx \Omega_\mu$. In addition, we only treat resonance with the ground ($1s$) state of an electron in a Coulomb potential having a nuclear charge $Z = 1$, corresponding to electron-proton BrS.

Taking these assumptions into account, we neglect the interference between resonant channels with different μ values as well as between resonant and potential parts of the BrS amplitude, so that the electron-nucleus BrS spectral density can be evaluated using the following approximation for the BrS spectral density:

$$\frac{d\sigma(\mathbf{p}_i,\Omega)}{d\Omega} \approx \frac{d\sigma^{(p)}(\mathbf{p}_i,\Omega)}{d\Omega} + \frac{2\hbar}{\pi\Gamma}\sum_{k=-\infty}^{\infty} \times \frac{\widetilde{\sigma}_{\mu+k}(\mathbf{p}_i)}{[2\hbar\Gamma^{-1}(\Omega_{\mu+k}-\Omega)]^2+1}. \quad (97)$$

Result (97) represents the sum of the nonresonant BrS cross section with resonant ones given by Eq. (39) for each particular Ω_μ. The potential part $d\sigma^{(p)}/d\Omega$ of the BrS cross section in Eq. (97) is evaluated using the low-frequency result, (50), in which we use the exact field-free Coulomb BrS cross section given in Ref. [16]. The total ionization rate Γ for the $1s$ state of the hydrogen atom is obtained using the analytic results in Ref. [31]. For the radiative recombination cross section $\widetilde{\sigma}_\mu$ in Eq. (97) we use the analytic result, (60), which in turn contains the exact field-free cross section $\widetilde{\sigma}^{(0)}$. For the case of a Coulomb potential, $\widetilde{\sigma}^{(0)}$ is well -known (e.g., cf. Ref. [32]).

The neglect of resonant channels with excited states of the H atom is justified by comparing $\widetilde{\sigma}^{(0)}$ for the $1s$ and $2s$ states, shown in Fig. 7: the cross section for radiative recombination into the ground state is more than an order of magnitude higher than that for recombination into the $2s$ excited state. Note that replacement of the exact cross section $\widetilde{\sigma}^{(0)}$ by its Born approximation counterpart $\widetilde{\sigma}^{(B)}$ can lead to a significant overestimate of the resonant enhancement of the BrS spectrum as shown in Fig. 7, in which $\widetilde{\sigma}^{(0)}$ and $\widetilde{\sigma}^{(B)}$ are compared. The Born approximation cross section $\widetilde{\sigma}^{(B)}$ results from approximating the initial electron state $\varphi_{\mathbf{p}_i}$ by the plane wave $\exp(i\mathbf{p}_i \cdot \mathbf{r}/\hbar)$. In the presence of a laser field, the Born approximation is widely used in studies of strong-laser processes (e.g., cf. Refs. [21–23] for the LARR process) and corresponds to replacing the QES $\Phi_{\mathbf{p}_i}$ by the Volkov wave $\chi_{\mathbf{p}_i}$, i.e., neglecting the interaction of the active electron with the scattering potential.

Numerical results for electron-proton BrS spectra in a laser field with $\lambda = 400$ nm (the second harmonic of a Ti:sapphire laser) and intensity $I = 1.67 \times 10^{14}$ W/cm^2 are shown in Fig. 8 for the case of an incident electron beam directed along the laser polarization axis, $\mathbf{p}_i \| \mathbf{e}_z$. One sees in Fig. 8 that the

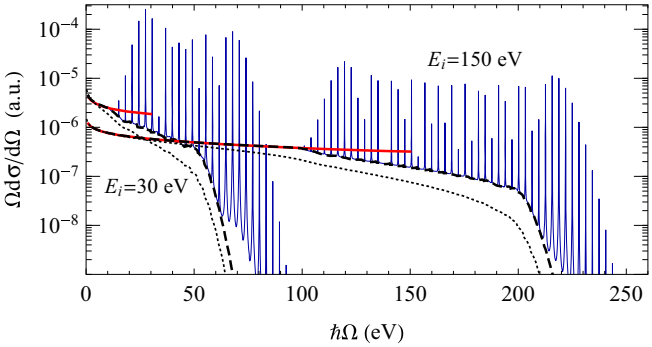

FIG. 8. (Color online) Spectral density of laser-assisted electron-proton BrS in a laser field with $\lambda = 400$ nm ($\hbar\omega = 3.1$ eV) and intensity $I = 1.67 \times 10^{14}$ W/cm^2 for electrons incident along the laser polarization axis, $\mathbf{p}_i \| \mathbf{e}_z$, at two energies: $E_i = 30$ eV and $E_i = 150$ eV. Thin solid (blue) lines—estimate using Eq. (97); dashed (black) lines—low-frequency result, (50); dotted (black) lines—Karapetyan-Fedorov result (cf. Ref. [1]); thick solid (red) lines—field-free BrS spectrum.

electron-proton BrS spectra exhibit all features exhibited in the results discussed above for resonant electron-atom BrS obtained using the TDER theory for the case of a short-range atomic potential, $U(r)$. For emitted photon frequencies $\Omega > \Omega_-^{(r)}$ the spectral density has pronounced resonant peaks, increasing $d\sigma/d\Omega$ by orders of magnitude. As the electron energy E_i increases, the positions of the resonant BrS peaks are shifted to higher values of Ω. The widths of the resonant peaks are independent of E_i and are equal to $\Gamma = 0.024$ eV for the laser field parameters we employ. The resonant enhancement of the BrS cross section is maximal (by a factor $\approx 8 \times 10^3$) beyond the plateau cutoff in the nonresonant BrS spectrum (i.e., for $\Omega > \Omega_{\max}^{(p)}$). For comparison we present in Fig. 8 the low-frequency result, (50), and the result of Karapetyan and Fedorov [1] for nonresonant electron-proton BrS. The latter result can be obtained from Eq. (50) by replacing the exact field-free BrS cross section, $d^2\sigma^{(0)}/d\Omega d\Omega_{\mathbf{p}_f}$, there with its Born approximation counterpart, $d^2\sigma^{(B)}/d\Omega d\Omega_{\mathbf{p}_f}$.

In order to compare the intensities of the resonant BrS spectral density with the nonresonant one, we average the resonant part of the BrS cross section in Eq. (97) over the frequency intervals $\Omega_\mu - \omega/2 < \Omega < \Omega_\mu + \omega/2$, using Eq. (41) (in which the integration limits are extended to $\pm\infty$ owing to the condition $\Gamma \ll \hbar\omega$). We thus obtain $\langle d\sigma^{(\mu)}/d\Omega\rangle \approx \tilde{\sigma}_\mu/\omega$. The recombination cross section $\tilde{\sigma}_\mu$ and the nonresonant BrS cross section are evaluated using Eqs. (60) and (54), respectively. The results are shown in Fig. 9, in which we present the spectral density for electron-proton BrS in a laser field with $\lambda = 400$ nm. Results for two different incident electron energies E_i and a fixed laser intensity I are compared in Fig. 9(a); results for two different laser intensities and a fixed incident energy E_i are compared in Fig. 9(b). The nonresonant BrS spectral density in Fig. 9 exhibits "stair-like" structures with "steps" at BrS photon energies $\hbar\Omega = E_i + k\hbar\omega$ (where k is an integer). These steps originate from the fact that with increasing Ω the partial BrS cross section with exchange of k photons [i.e., the term with $n = k$ in Eqs. (10) or (50)] does not contribute to the sum over n for the BrS spectral density. The

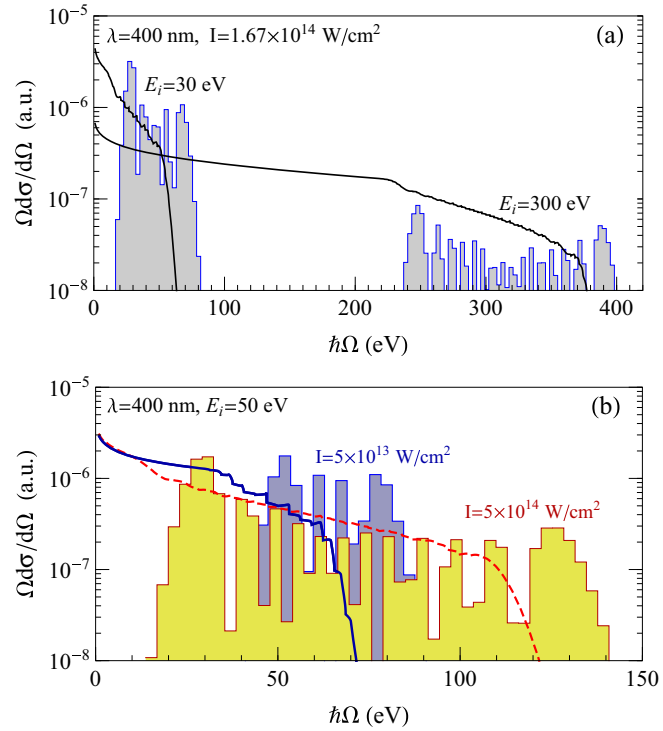

FIG. 9. (Color online) Comparison of curves for the *nonresonant* laser-assisted electron-proton BrS spectral density [obtained using Eq. (50)] with histograms for the *resonant* laser-assisted electron-proton BrS spectral density for a laser field with $\lambda = 400$ nm ($\hbar\omega = 3.01$ eV). Each bar in the histograms for the resonant spectral densities represents an average over the interval $\Omega_\mu - \omega/2 < \Omega < \Omega_\mu + \omega/2$ about the μth resonance peak. (a) Results for two incident electron energies, $E_i = 30$ and 300 eV, and laser intensity $I = 1.67 \times 10^{14}$ W/cm^2. (b) Results for $E_i = 50$ eV and two laser intensities: $I = 5 \times 10^{13}$ W/cm^2 [solid (blue) line and dark (blue) bars] and $I = 5 \times 10^{14}$ W/cm^2 [dashed (red) line and light (yellow) bars].

stair-like structure is clearly visible for the lowest intensity, $I = 5 \times 10^{13}$ W/cm^2, in which case the integer k varies from -5 to 6 with increasing Ω.

As the results in Fig. 9 show, with either increasing electron energy E_i or increasing laser intensity I, the averaged resonant BrS spectral density becomes broader and decreases more rapidly than that for the nonresonant case. This broadening and decreasing magnitude of the spectral density for resonant BrS stem from the behavior of the generalized Bessel function J_μ in Eq. (60) for the LARR cross section and in Eq. (59) for the Fourier component (or QES harmonic) $c_\mu(\mathbf{p}_i)$ of the incident electron QES at the origin, $\chi_{\mathbf{p}_i}(\mathbf{r} = 0, t)$. Physically, the coefficient $c_k(\mathbf{p}_i)$ determines the population of the QES harmonic corresponding to k-photon exchange with the laser field. With increasing incident electron energy or laser intensity, the number of populated QES harmonics increases, while only one of them (with $k = \mu$) contributes to the resonant BrS cross section. The redistribution of the incident electron density over a larger number of QES harmonics leads to a decrease in $|c_\mu(\mathbf{p}_i)|$ and hence in the resonant BrS cross section. In contrast, for potential (nonresonant) BrS, the entire set of QES harmonics in open channels (i.e., with $\epsilon_i + k\hbar\omega - \hbar\Omega > 0$) contributes to the cross section [cf. Eq. (50)].

Considering the integrated spectral density of resonant BrS over the entire interval of emitted photon energies (indicated by the shaded areas in Fig. 9), we conclude that the contributions of the resonant channels to the total spontaneous radiation intensity increases with increasing I and with decreasing E_i.

VI. SUMMARY AND CONCLUSIONS

In this paper, we have analyzed the key features of resonant phenomena in spontaneous laser-assisted BrS caused by the possibility that the scattering electron may be virtually captured in a quasibound state of the target potential. In the vicinity of resonant energies of the BrS photon, $\hbar\Omega_\mu = p_i^2/(2m) + u_p + |\mathrm{Re}\,\varepsilon| + \mu\hbar\omega$ (which coincide with the photon energies of the LARR or LARA process), the BrS spectra exhibit resonant peaks, which significantly increase the BrS cross section. The shape of the resonant BrS spectrum at $\Omega = \Omega_\mu$ coincides with that of the spectrum for LARR or LARA.

The key result of this paper is the general parametrization, (35), for the resonant BrS partial cross section, corresponding to exchange of n laser photons and spontaneous emission of the BrS photon $\hbar\Omega_\mu$ during electron-atom scattering. Result (35) has a transparent physical meaning, representing the BrS cross section as a product of three factors: (i) the LARR or LARA cross section $\widetilde{\sigma}_\mu(\mathbf{p}_i)$ describes the transition of the incident electron with momentum $\mathbf{p}_i$ from the continuum (scattering) state to the bound quasistationary state with spontaneous radiation of $\hbar\Omega_\mu$; (ii) the ATI or ATD rate $dR(\mathbf{p}_\nu)/d\Omega_{\mathbf{p}_\nu}$ describes a ν-photon ($\nu = n - \mu$) transition from the bound state to the continuum state of the electron with final momentum $\mathbf{p}_f = \mathbf{p}_\nu$; and (iii) the resonant profile function $\sim(1 + \mathrm{Im}\,q + \delta\mathrm{Re}\,q)/(\delta^2 + 1)$ describes the dependence of the BrS cross section on the emitted photon energy $\hbar\Omega$ in the vicinity of the resonant energy $\hbar\Omega_\mu$. In general, result (35) describes an asymmetric profile of the resonant peak that is similar to the Fano profile in photoionization cross sections [8–10]. The asymmetry parameter q is expressed in terms of the nonresonant $\mathbf{d}_n^{(p)}$ and resonant $\mathbf{d}_n^{(r)}$ parts of the BrS amplitude [cf. Eq. (38)]. It is worth noting that the parameter q involves the scalar product of the complex vectors $\mathbf{d}_n^{(p)}$ and $\mathbf{d}_n^{(r)}$. It thus encompasses a wide variety of resonance profiles, depending on the parameters of the problem.

The key ingredients of the resonant BrS cross section may be evaluated either numerically or analytically within the low-frequency approximation. In order to confirm the accuracy of the general parametrization of the resonant BrS cross section, we have adapted the TDER theory to treat the laser-assisted BrS process. Our numerical results show that (for the case of e-H BrS in a CO_2 laser field) the results obtained using the low-frequency closed-form analytic expressions are in excellent agreement with the results obtained using the exact equations of the TDER theory.

Neglecting the interference between different resonant channels, as well as between resonant and potential parts of the BrS amplitude (i.e., omitting details of the resonant peak profiles), we have found that for the case of a long-range electron-Coulomb interaction (i.e., for electron-proton BrS) the resonant features in the BrS cross section are similar to those for a short-range atomic potential.

Considering the BrS cross section as a function of the final electron momentum (i.e., of the scattered electron energy and direction), we have found that the main contribution to the BrS spectral density at resonant energies is given by low-energy electrons ($E_f \lesssim 2u_p$) that are scattered along the laser polarization direction. This result can be explained by the energy and angular dependence of the ionization or detachment rate of the virtually captured electron. It is remarkable that for electron scattering at small angles, the resonant BrS spectrum is significantly wider than the nonresonant one, so that for high energies $\hbar\Omega$ the BrS spectrum is described essentially entirely by the resonant BrS spectral density. Our results show also that the contribution of the resonant channel to laser-assisted electron BrS is sensitive to the incident electron energy E_i and to the laser intensity I: increasing E_i or I leads to a broadening of the BrS spectrum, within which resonance peaks are pronounced features; simultaneously, the averaged resonant BrS spectral density decreases.

Finally, we note that rescattering effects in laser-assisted BrS are not significant for the laser parameters and incident electron energies used in this paper. However, for lower electron energies E_i and higher laser intensities (when $E_i \ll u_p$), rescattering effects become significant and lead to the appearance of a second, high-energy (rescattering) plateau in the BrS spectrum, similarly to the occurrence of rescattering plateaus in laser-assisted electron-atom scattering [27,34] and LARR or LARA processes [19,22]. Also, rescattering effects become important when the incident electron quasienergy is resonant with a bound state of the target (i.e., $\epsilon_i - k\hbar\omega = \mathrm{Re}\,\varepsilon$, where k is a positive integer). A detailed analysis of the role of rescattering (as well as laser polarization) effects in BrS will be published elsewhere.

ACKNOWLEDGMENTS

This work was supported in part by RFBR Grants No. 13-02-00420 and No. 14-02-31412_young_a, by NSF Grant No. PHYS-1208059, and by the Ministry of Education and Science of the Russian Federation (Project No. 1019).

APPENDIX: DERIVATION OF THE TDER EXPRESSION FOR THE BRS DIPOLE MATRIX ELEMENT $\mathbf{d}_n$

Because the scattering state, (63), is comprised of two terms, an incident plane wave, $\chi_{\mathbf{p}}$, and a scattered wave (either $\Phi_{\mathbf{p}}^{(+)}$ or $\Phi_{\mathbf{p}}^{(-)}$), we write the BrS dipole matrix element $\mathbf{d}_n$ as the sum of four terms [cf. Eq. (71)]:

$$\mathbf{d}_n(\mathbf{p}_i,\mathbf{p}_f) = \sum_{k=0}^{3} \mathbf{d}_n^{(k)}, \quad \mathbf{d}_n^{(k)} = \frac{1}{T}\int_0^T dt e^{in\omega t}\mathbf{d}^{(k)}(t).$$

Let us consider each of these terms separately.

The dipole moment $\mathbf{d}^{(0)}(t) = \langle\chi_{\mathbf{p}_f}(t)|\mathbf{d}|\chi_{\mathbf{p}_i}(t)\rangle$ represents a dipole transition between the Volkov states $\chi_{\mathbf{p}_i}(\mathbf{r},t)$ and $\chi_{\mathbf{p}_f}(\mathbf{r},t)$ of a free electron in the laser field $\mathbf{F}(t)$. Using the explicit form of $\chi_{\mathbf{p}}(\mathbf{r},t)$ in Eq. (14) and the following relation for the Dirac δ function, $\int \mathbf{r}e^{i\mathbf{kr}}d\mathbf{r} = -i(2\pi)^3\nabla_{\mathbf{k}}\delta(\mathbf{k})$,

we obtain, for $\mathbf{d}^{(0)}(t)$,

$$\mathbf{d}^{(0)}(t) = i(2\pi)^3\hbar^4 e \exp\left[\frac{ie}{\hbar m\omega^2}\mathbf{F}(t)\cdot(\mathbf{p}_i - \mathbf{p}_f)\right] \times \nabla_{\mathbf{p}_f}\delta(\mathbf{p}_i - \mathbf{p}_f). \tag{A1}$$

The Fourier transform of Eq. (A1), corresponding to $\Omega = n\omega > 0$, leads to result (75),

$$\mathbf{d}_n^{(0)} = 4(\pi\hbar)^3\frac{e^2\mathbf{F}}{m\omega^2}\cdot(\mathbf{p}_i - \mathbf{p}_f)\nabla_{\mathbf{p}_f}\delta(\mathbf{p}_f - \mathbf{p}_i)\delta_{n,1} = 4(\pi\hbar)^3\frac{e^2\mathbf{F}}{m\omega^2}\delta(\mathbf{p}_f - \mathbf{p}_i)\delta_{n,1}, \tag{A2}$$

where the relation $x\delta'(x) = -\delta(x)$ has been used.

The terms $\mathbf{d}^{(1)}(t) = \langle\Phi_{\mathbf{p}_f}^{(-)}(t)|\mathbf{d}|\chi_{\mathbf{p}_i}(t)\rangle$ and $\mathbf{d}^{(2)}(t) = \langle\chi_{\mathbf{p}_f}(t)|\mathbf{d}|\Phi_{\mathbf{p}_i}^{(+)}(t)\rangle$ are expressed in terms of the advanced, $G^{(-)}$, and retarded, $G^{(+)}$, Green's functions for a free electron in the field $\mathbf{F}(t)$, as follows:

$$\mathbf{d}^{(1)}(t) = -\frac{2\pi e\hbar^2}{m\kappa}\int_t^\infty dt' e^{i\epsilon_f(t'-t)/\hbar} f_{-\mathbf{p}_f}(-t') \times \int d\mathbf{r}\chi_{\mathbf{p}_i}(\mathbf{r},t)\mathbf{r}G^{(-)*}(\mathbf{r},t;0,t')dt', \tag{A3}$$

$$\mathbf{d}^{(2)}(t) = -\frac{2\pi e\hbar^2}{m\kappa}\int_{-\infty}^t dt' e^{i\epsilon_i(t-t')/\hbar} f_{\mathbf{p}_i}(t') \times \int d\mathbf{r}\chi_{\mathbf{p}_f}^*(\mathbf{r},t)\mathbf{r}G^{(+)}(\mathbf{r},t;0,t')dt'. \tag{A4}$$

For $G^{(\pm)}(\mathbf{r},t;\mathbf{r}',t')$ we use the well-known Feynman form,

$$G^{(\pm)}(\mathbf{r},t;\mathbf{r}',t') = \mp\theta[\pm(t-t')]\frac{i}{\hbar}\left[\frac{m}{2\pi i\hbar(t-t')}\right]^{3/2} \times \exp[iS(\mathbf{r},t;\mathbf{r}',t')/\hbar], \tag{A5}$$

where $\theta(x)$ is the Heaviside function and S is the classical action for an electron in the laser field $\mathbf{F}(t)$:

$$S(\mathbf{r},t;\mathbf{r}',t') = \frac{m}{2(t-t')}\left(\mathbf{r} - \mathbf{r}' + \frac{e}{m\omega^2}[\mathbf{F}(t) - \mathbf{F}(t')]\right)^2 - \frac{e^2}{2mc^2}\int_{t'}^t \mathbf{A}^2(\tau)d\tau - \frac{e}{c}[\mathbf{r}\cdot\mathbf{A}(t) - \mathbf{r}'\cdot\mathbf{A}(t')]. \tag{A6}$$

Using Eqs. (A5) and (A6) and the explicit form for $\chi_{\mathbf{p}}(t)$ in Eq. (14), straightforward integration of the spatial integrals in Eqs. (A3) and (A4) gives

$$\mathbf{d}^{(1)}(t) = \frac{2\pi ie\hbar}{m^2\kappa}\int_{-\infty}^0 d\tau\left(\mathbf{p}_i\tau - \frac{e}{\omega^2}[\mathbf{F}(t) - \mathbf{F}(t-\tau)]\right) \times f_{-\mathbf{p}_f}(\tau - t)e^{i[(\epsilon_i-\epsilon_f)\tau + S_{\mathbf{p}_i}(t-\tau)]/\hbar}, \tag{A7}$$

$$\mathbf{d}^{(2)}(t) = \frac{2\pi ie\hbar}{m^2\kappa}\int_0^\infty d\tau\left(\mathbf{p}_f\tau - \frac{e}{\omega^2}[\mathbf{F}(t) - \mathbf{F}(t-\tau)]\right) \times f_{\mathbf{p}_i}(t-\tau)e^{i[(\epsilon_i-\epsilon_f)\tau - S_{\mathbf{p}_f}(t-\tau)]/\hbar}. \tag{A8}$$

Since the functions $f_{\mathbf{p}}(t)$ and $S_{\mathbf{p}}(t)$ are periodic in t, we evaluate the integrals over τ in Eqs. (A7) and (A8) using the Fourier expansions,

$$f_{\mathbf{p}_i}(t-\tau)e^{-iS_{\mathbf{p}_f}(t-\tau)/\hbar} = \sum_k e^{-ik\omega(t-\tau)}\mathcal{L}_k^{(2)},$$

$$f_{-\mathbf{p}_f}(\tau - t)e^{iS_{\mathbf{p}_i}(t-\tau)/\hbar} = \sum_k e^{-ik\omega(t-\tau)}\mathcal{L}_k^{(1)},$$

and the regularization rule,

$$\int_0^{\pm\infty} d\tau e^{i\alpha\tau} = \lim_{\gamma\to\pm 0}\int_0^{\pm\infty} d\tau e^{i\alpha\tau-\gamma\tau} = \frac{i}{\alpha}.$$

Subsequent integration over t gives the following results for $\mathbf{d}_n^{(1,2)}$:

$$\mathbf{d}_n^{(1)} = C\left(2i\frac{\omega\mathbf{p}_i}{eF}\mathcal{L}_n^{(1)} + \mathbf{e}_z\sum_{s=\pm 1}\frac{\mathcal{L}_{n+s}^{(1)}}{\omega/\Omega + s}\right), \tag{A9}$$

$$\mathbf{d}_n^{(2)} = -C\left(2i\frac{\omega\mathbf{p}_f}{eF}\mathcal{L}_n^{(2)} + \mathbf{e}_z\sum_{s=\pm 1}\frac{\mathcal{L}_{n+s}^{(2)}}{\omega/\Omega + s}\right), \tag{A10}$$

where $C = \pi\hbar e^2F/(\kappa m^2\Omega^2\omega)$.

Finally, for the dipole moment $\mathbf{d}^{(3)}(t)$ we have

$$\mathbf{d}^{(3)}(t) = e\left(\frac{2\pi\hbar^2}{m\kappa}\right)^2\int_{-\infty}^t dt'\int_t^\infty dt'' \times e^{i[\epsilon_i(t-t')+\epsilon_f(t''-t)]/\hbar} f_{\mathbf{p}_i}(t')f_{-\mathbf{p}_f}(-t'') \times \int d\mathbf{r}\, G^{(+)}(\mathbf{r},t;0,t')\,\mathbf{r}\,G^{(-)*}(\mathbf{r},t;0,t''). \tag{A11}$$

For the spatial integral in Eq. (A11) we use the relation (cf., e.g., the Appendix in Ref. [33])

$$\int d\mathbf{r}\, G^{(+)}(\mathbf{r},t;0,t')\,\mathbf{r}\,G^{(-)*}(\mathbf{r},t;0,t'') = \frac{i}{\hbar}G^{(+)}(0,t'';0,t')\boldsymbol{\mathcal{R}}(t;t',t''),$$

where

$$\boldsymbol{\mathcal{R}}(t;t',t'') = \frac{e}{m\omega^2(t'-t'')}\{(t-t'')[\mathbf{F}(t) - \mathbf{F}(t')] - (t-t')[\mathbf{F}(t) - \mathbf{F}(t'')]\}.$$

To evaluate the double integral over the times t' and t'' in Eq. (A11) we introduce new variables,

$$\xi = t'' - t', \quad \zeta = 2t - t' - t'',$$

where $0 \le \xi < \infty$, $-\xi \le \zeta \le \xi$. In the new variables, the integration over ζ is carried out analytically. As a result, the Fourier components $\mathbf{d}_n^{(3)}$ of $\mathbf{d}^{(3)}(t)$ may be expressed in terms of one-dimensional integrals $W_{k,k'}$ over $\phi = \xi\omega/2$ [cf. Eq. (81)]:

$$\mathbf{d}_n^{(3)} = \mathbf{e}_z C\sum_{k,k'} W_{k,k'} f_k(\mathbf{p}_i)f_{k-n+1+2k'}(-\mathbf{p}_f). \tag{A12}$$

Combining results (A2), (A9), (A10), and (A12), we obtain the final result for the dipole matrix element $\mathbf{d}_n(\mathbf{p}_i,\mathbf{p}_f)$, given by Eq. (74).

[1] R. V. Karapetyan and M. V. Fedorov, Zh. Eksp. Teor. Fiz. **75**, 816 (1978) [Sov. Phys. JETP **48**, 412 (1978)].

[2] F. Zhou and L. Rosenberg, Phys. Rev. A **48**, 505 (1993).

[3] N. M. Kroll and K. M. Watson, Phys. Rev. A **8**, 804 (1973).

[4] F. Ehlotzky, A. Jaroń, and J. Z. Kamiński, Phys. Rep. **297**, 63 (1998).

[5] M. Dondera and V. Florescu, Rad. Phys. Chem. **75**, 1380 (2006).

[6] A. V. Flegel, M. V. Frolov, N. L. Manakov, and A. F. Starace, Phys. Rev. Lett. **102**, 103201 (2009).

[7] A. N. Zheltukhin, A. V. Flegel, M. V. Frolov, N. L. Manakov, and A. F. Starace, J. Phys. B **45**, 081001 (2012).

[8] U. Fano, Phys. Rev. **124**, 1866 (1961).

[9] U. Fano and J. W. Cooper, Rev. Mod. Phys. **40**, 441 (1968), sec. 8.1.

[10] A. F. Starace, Phys. Rev. A **16**, 231 (1977).

[11] E. Lötstedt, U. D. Jentschura, and C. H. Keitel, Phys. Rev. Lett. **98**, 043002 (2007).

[12] S. Schnez, E. Lötstedt, U. D. Jentschura, and C. H. Keitel, Phys. Rev. A **75**, 053412 (2007).

[13] A. A. Lebed' and S. P. Roshchupkin, Phys. Rev. A **81**, 033413 (2010).

[14] S. P. Roshchupkin, A. A. Lebed', E. A. Padusenko, and A. I. Voroshilo, Laser Phys. **22**, 1113 (2012).

[15] N. L. Manakov, V. D. Ovsiannikov, and L. P. Rapoport, Phys. Rep. **141**, 319 (1986).

[16] L. D. Landau and E. M. Lifshitz, *Quantum Electrodynamics: Course of Theoretical Physics*, 2nd ed. (Pergamon, Oxford, UK, 1982).

[17] N. L. Manakov and A. G. Fainshtein, Teor. Mat. Fiz. **48**, 375 (1981) [Theor. Math. Phys. **48**, 815 (1981)].

[18] N. L. Manakov, M. V. Frolov, A. F. Starace, and I. I. Fabrikant, J. Phys. B **33**, R141 (2000).

[19] A. N. Zheltukhin, N. L. Manakov, A. V. Flegel, and M. V. Frolov, Pis'ma Zh. Eksp. Teor. Fiz. **94**, 641 (2011) [JETP Lett. **94**, 599 (2011)].

[20] M. Abramowitz and I. A. Stegun (eds.), *Handbook of Mathematical Functions* (Dover, New York, 1965).

[21] M. Yu. Kuchiev and V. N. Ostrovsky, Phys. Rev. A **61**, 033414 (2000).

[22] D. B. Milošević and F. Ehlotzky, Phys. Rev. A **65**, 042504 (2002).

[23] A. Jaroń, J. Z. Kamiński, and F. Ehlotzky, Phys. Rev. A **61**, 023404 (2000).

[24] L. V. Keldysh, Zh. Eksp. Teor. Fiz. **47**, 1945 (1964) [Sov. Phys. JETP **20**, 1307 (1965)].

[25] V. S. Popov, Usp. Fiz. Nauk **174**, 921 (2004) [Phys. Usp. **47**, 855 (2004)].

[26] N. L. Manakov, A. F. Starace, A. V. Flegel, and M. V. Frolov, Pis'ma Zh. Eksp. Teor. Fiz. **87**, 99 (2008) [JETP Lett. **87**, 92 (2008)].

[27] A. V. Flegel, M. V. Frolov, N. L. Manakov, A. F. Starace, and A. N. Zheltukhin, Phys. Rev. A **87**, 013404 (2013).

[28] A. V. Flegel, M. V. Frolov, N. L. Manakov, and A. N. Zheltukhin, J. Phys. B **42**, 241002 (2009).

[29] M. V. Frolov, N. L. Manakov, and A. F. Starace, Phys. Rev. A **78**, 063418 (2008).

[30] M. V. Frolov, N. L. Manakov, E. A. Pronin, and A. F. Starace, Phys. Rev. Lett. **91**, 053003 (2003).

[31] S. V. Popruzhenko, V. D. Mur, V. S. Popov, and D. Bauer, Phys. Rev. Lett. **101**, 193003 (2008).

[32] I. I. Sobelman, *Atomic Spectra and Radiative Transitions*, 2nd ed. (Springer, Berlin, 1996).

[33] M. V. Frolov, A. V. Flegel, N. L. Manakov, and A. F. Starace, Phys. Rev. A **75**, 063407 (2007).

[34] N. L. Manakov, A. F. Starace, A. V. Flegel, and M. V. Frolov, Pis'ma Zh. Eksp. Teor. Fiz. **76**, 316 (2002) [JETP Lett. **76**, 258 (2002)].